

2 **Molecular Landscape of Anti-Drug Antibodies Reveals the Mechanism of the Immune**
3 **Response Following Treatment with TNF α Antagonists**

4 *Running title: Molecular landscape of anti-drug antibodies*

5 ^{1,†}Anna Vaisman-Mentesh, ^{1,†}Shai Rosenstein, ²Miri Yavzori, ¹Yael Dror, ²Ella Fudim,
6 ²Bella Ungar, ²Uri Kopylov, ²Orit Picard, ¹Aya Kigel, ²Shomron Ben-Horin, ¹Itai Benhar,
7 ^{1,*}Yariv Wine

8
9 ¹George S. Wise Faculty of Life Sciences, School of Molecular Cell Biology and Biotechnology,
10 Tel Aviv University, Ramat Aviv, Israel

11 ²Gastroenterology Department, Sheba Medical Center and Sackler School of Medicine, Tel-Aviv
12 University, Tel Hashomer, Israel

13 [†] These authors have contributed equally to this work.

14 *Author for correspondence: Yariv Wine

15 yarivwine@tauex.tau.ac.il

16
17 **Keywords:** Immunogenicity, anti-drug antibodies, next generation sequencing, Ig-Seq, BCR-Seq,
18 immune repertoire, antibody repertoire, proteomics, high-throughput sequencing, monoclonal
19 antibody, biologics, therapeutic antibodies

20

21 **Abstract**

22
23 Drugs formulated from monoclonal antibodies (mAbs) are clinically effective in various diseases.
24 Repeated administration of mAbs, however, elicits an immune response in the form of anti-drug-
25 antibodies (ADA), thereby reducing the drug's efficacy. Notwithstanding their importance, the
26 molecular landscape of ADA and the mechanisms involved in their formation are not fully
27 understood. Using a newly developed quantitative bio-immunoassay, we found that ADA
28 concentrations specific to TNF α antagonists can exceed extreme concentrations of 1 mg/ml with
29 a wide range of neutralization capacity. Our data further suggest a preferential use of the λ light
30 chain in a subset of neutralizing ADA. Moreover, we show that administration of TNF α
31 antagonists result in a vaccine-like response whereby ADA formation is governed by the
32 extrafollicular T cell-independent immune response. Our bio-immunoassay coupled with insights
33 on the nature of the immune response can be leveraged to improve mAb immunogenicity
34 assessment and facilitate improvement in therapeutic intervention strategies.

35
36

37 **MAIN TEXT**

38

39 **Introduction**

40 More than 30 years since the approval of the first therapeutic monoclonal antibody (mAb) for
41 clinical use, the therapeutic mAb market has expanded exponentially, establishing mAbs as one of
42 the leading biopharmaceutical therapeutic modalities (1). Although mAbs hold significant
43 promise for improving human health, their repeated administration is often highly immunogenic
44 and can elicit an undesirable anti-drug antibody (ADA) response (2). The formation of an ADA
45 response interferes with the effect of the drug or neutralizes it thereby altering the drug's
46 pharmacokinetic (PK) and pharmacodynamic (PD) properties and reducing its efficacy (3), and
47 eventually may lead to a severe adverse immune reaction in humans (4).

48 Immunogenicity of mAbs and the formation of an ADA response has been suggested to be
49 dependent on the interplay between factors related to the drug itself (e.g., non-human sequence,
50 glycosylation, impurities, aggregation), to the patient (e.g., disease type, genetic factors,
51 concomitant immunomodulators), or to the drug's route and frequency of administration (5, 6).
52 However, the molecular mechanisms that lead to the induction of ADA are not well understood
53 and were initially thought to be related to the murine origin of the mAbs because they were
54 recognized as "non-self" by the human immune system. This idea propelled the mAb discovery
55 field to focus on engineering refined mAbs by reducing the nonhuman portions and developing
56 chimeric, humanized, and fully human mAbs by using human libraries or humanized mice at the
57 mAb discovery phase (7).

58 Unfortunately, this strategy did not abolish the immunogenicity potential of mAbs and the
59 associated induction of ADA. The question of why and how ADA develop is further complicated
60 by data indicating that some patients develop ADA, and some do not, and by the observation that
61 the extent of immunogenicity may differ among patients receiving the same mAb (8). ADA that
62 develop in patients treated with an mAb can be stratified into two main categories: 1) neutralizing
63 ADA (*nt*ADA) that directly block and interfere with the drug's ability to bind its target, and 2)
64 non-neutralizing ADA (i.e., binding ADA *b*ADA) that recognize other epitopes on the drug while
65 still retaining the mAb binding activity (9). *nt*ADA are generally considered to be more important
66 in the clinical setting than *b*ADA because they directly reduce a drug's efficacy. However, *b*ADA
67 may indirectly reduce the therapeutic efficacy of an mAb by compromising bioavailability or

68 accelerating drug clearance from the circulation. In both cases, *nt*ADA and *b*ADA substantially
69 alter the PK and PD of the mAb being administered (10).

70 Originator and biosimilar tumor necrosis factor alpha (TNF α) antagonistic mAbs are used
71 extensively in clinical settings to treat inflammatory bowel disease (IBD; e.g., Crohn's disease
72 and ulcerative colitis), rheumatoid arthritis, and other chronic inflammatory associated disorders
73 such as psoriasis, psoriatic arthritis, and ankylosing spondylitis (11). TNF α antagonists help
74 reduce inflammatory responses by targeting both membrane-bound and soluble TNF α .
75 Neutralizing soluble TNF α prevents its binding to its receptor and impedes the secretion and
76 upregulation of the signal cascade, thereby inhibiting its biological activity. The binding of TNF α
77 antagonists to transmembrane TNF α on immune effector cells causes their destruction by
78 inducing cell apoptosis or cell lysis through reverse signaling (12).

79 Currently, five TNF α antagonists have been approved by both the U.S. Food and Drug
80 Administration and the European Medicines Agency: infliximab (IFX), adalimumab (ADL),
81 etanercept, golimumab, and certolizumab pegol (2). Additionally, several biosimilars have
82 already been approved or are in various stages of development (13). Both IFX and ADL belong to
83 the group of TNF α antagonists and are routinely used in clinical settings to treat inflammatory
84 diseases. IFX is a chimeric mAb (75% human and 25% murine), whereas ADL is fully human.
85 The reported immunogenicity extent of these drugs is inconsistent. Whereas pharmaceutical
86 companies report 10–15% and 2.6–26% immunogenicity for IFX and ADL, respectively (14),
87 clinical data suggest higher immunogenicity rates for these drugs (15). Patients treated with IFX
88 and ADL can be stratified based on the characteristics of their response to treatment or lack
89 thereof. Primary non-responders are patients whose disease does not respond to the drug at all,
90 and a certain subset of these may be mediated via early formation of ADA (15, 16). Secondary
91 non-responders are patients who initially respond to the drug but later fail treatment, often due to
92 development of ADA (for IFX, this was reported to develop mostly within 12 months of
93 treatment initiation) (16).

94 Studies reporting immunogenicity following mAb administration and ADA prevalence have been
95 inconsistent due in part to the various assay formats used to monitor immunogenicity in the clinic
96 (17). Current limitations of each available format might reduce utility in clinical and research
97 settings and complicate data interpretation. Some assays have a poor dynamic range and may
98 generate false negative results because of interfering interaction with another circulating drug, or
99 conversely, false positive results due to the presence of other antibodies such as rheumatoid factor

100 (18). The pros and cons of available ADA detection assays were previously elaborated, and the
101 formation of ADA following treatment with IFX, ADL, and other TNF α antagonists, including
102 newly developed biosimilars, have been extensively studied and reviewed elsewhere (5, 19-21).
103 Notwithstanding the effort invested in understanding the reasons that mAb immunogenicity and
104 strategies to increase mAb efficacy, little is known about the molecular mechanism that governs
105 the formation of ADA following treatment with an mAb.

106
107 In this study, we investigated the molecular landscape of ADA following treatment with
108 TNF α antagonists. First, we developed a simple bio-immunoassay that accurately quantifies ADA
109 levels in patient sera. We further modified the bio-immunoassay to evaluate the neutralization
110 capacity of the ADA. Next, we aimed to profile the immune response following mAb
111 administration. We used flow cytometry to determine the frequency of B cells in the circulation
112 and whether the dynamics of the immune response was akin to vaccine response. Finally, we used
113 next-generation sequencing (NGS) and high-resolution shotgun tandem mass spectrometry (LC-
114 MS/MS) to elucidate the molecular composition of serum ADA. Using our bio-immunoassay we
115 found that ADA levels in sera from 55 patients ranged between 2.7 and 1,268.5 $\mu\text{g/ml}$. The
116 modified bio-immunoassay enabled us to differentiate between patients who have high and low
117 neutralization capacity. Interestingly, we found that patients with a high neutralization capacity
118 showed a strong bias in the λ/κ light chain ratio thereby suggesting that *ntADA* exhibits a
119 preference for λ light chains.

120 To elucidate the nature of the immune response following drug administration we chose to study a
121 patient with IBD who was treated with IFX and who had high ADA levels and neutralization
122 capacity. At 10 days (D10) following IFX infusion, the patient exhibited an approximately 13-
123 fold increase in the frequency of plasmablasts (PB) and unchanged frequency of activated
124 memory B cells (mBC), compared with the pre-infusion time point (D0). Comparative NGS
125 analysis of the antibody heavy chain variable region (V_H) from isolated PB at D0 and D10,
126 showed a significant temporal decrease in the level of somatic hypermutation (SHM) and an
127 increase in the length of the complementary determining region 3 of the antibody heavy chain
128 (CDRH3). Moreover, the proteomic analysis of serum ADA supports the observation obtained
129 from the neutralization capacity assays, that a preference for using λ light chains exists. These
130 data suggest a possible mechanism whereby the humoral immune response following the
131 administration TNF α antagonists is governed by a T cell-independent (TI) response. This
132 response may be induced by the formation of immunocomplexes (drug-TNF α -ADA) serving as a

133 strong driver of immunogenicity that in-turn diverts the immune response to TI pathway were B
134 cells are activated by B cell receptor (BCR) cross-linking.

135 **Materials and Methods**

136 **Over expression and purification of rhTNF α**

137 The sequence-encoding residues Val77–Leu233 of human TNF α was cloned and fused to the N-
138 terminal 6xHis tag in pET-28a+ vector (Novagen) and transformed into *Escherichia coli* Rosetta
139 (DE3) cells (Novagen). A single colony was inoculated into 2ml LB supplemented with
140 Kanamycin at final concentration of 100 μ g/ml and incubated over night (O.N.) at 37°C, 250
141 RPM. The culture was next re-inoculated into a 0.5L Erlenmeyer containing LB supplemented
142 with Kanamycin, and grown at 37°C 250RPM until O.D.₆₀₀~0.6-0.8 was reached. Induction was
143 carried out by supplementing bacterial culture with IPTG (0.1mM final concentration) and
144 incubating the culture for 3 hours at 37°C, 250RPM. Bacterial cells were harvested by
145 centrifugation at 8000 RPM, 15 minutes, at 10°C (SORVALL RC6 Plus, Thermo Fisher
146 Scientific) and cell pellet was stored O.N. at -20°C. Next, pellet was re-suspended in 30ml of
147 binding buffer (50mM sodium phosphate buffer pH 8.0, 300mM NaCl, 10mM imidazole) and
148 sonicated on ice for 8 cycles of 30 seconds pulse with 2-minute pause (W-385 sonicator, Heat
149 Systems Ultrasonics). Following sonication, cells were centrifuged at 12000 RPM, 30 minutes,
150 4°C (SORVALL RC 6+) and supernatant was applied to a HisTrap affinity column (GE
151 Healthcare) that was pre-equilibrated with binding buffer. All affinity purification steps were
152 carried out by connecting the affinity column to a peristaltic pump with flow rate of 1/ml/min.
153 Column was washed with 5 column volumes (CV) of wash buffer (50mM Sodium phosphate, pH
154 8.0, 300mM NaCl, 10% glycerol, 20mM imidazole) followed by elution of rhTNF α with 5CV of
155 elution buffer (50mM Sodium phosphate, pH 6.0, 300mM NaCl, 10% glycerol, 500mM
156 imidazole). Elution was collected in 1ml fractions and were analyzed by 12% SDS–PAGE.
157 Fractions containing clean rhTNF α were merged and dialyzed using Amicon Ultra (Mercury)
158 cutoff 3K against PBS (pH 7.4). Dialysis products were analyzed by 12% SDS–PAGE for purity
159 and concentration was measured using Take-5 (BioTek Instruments). To test functionality of the
160 produced rhTNF α , 96 well plate (Nunc MaxiSorp™ flat-bottom, Thermo Fisher Scientific) was
161 coated with 1 μ g/ml (in PBS) of purified rhTNF α and commercial hTNF α (PHC3011, Thermo
162 Fisher Scientific) and incubated at 4°C O.N. ELISA plates were then washed three times with
163 PBST (0.1% v/v Tween 20 in PBS) and blocked with 300 μ l of 2% w/v BSA in PBS for 1 hour at
164 37°C. Next, ELISA plates were washed three time with PBST, and incubated for 1 hour, room

165 temperature (RT) in triplicates with anti-TNF α mAb (Infliximab or Adalimumab) in 2% w/v
166 BSA, PBS at the starting concentration of 50nM with 3-fold dilution series. Plates were then
167 washed three times with PBST with 30 second incubation time at each washing cycle. For
168 detection, 50 μ l of anti-human H+L HRP conjugated antibody (Jackson) was added to each well
169 (1:5000 ratio in 2% w/v BSA in PBS) and incubated for 1 hour at RT, followed by three washing
170 cycles with PBST. Developing was carried out by adding 50 μ l of 3,3',5,5'-Tetramethylbenzidine
171 (TMB, Southern Biotech) and reaction was quenched by adding 50 μ l 0.1M sulfuric acid. Plates
172 were read using the Epoch Microplate Spectrophotometer ELISA plate reader (BioTek
173 Instruments).

174 **Over expression and purification of IdeS**

175 The coding sequence corresponding to amino acid residues 38–339 of *S. pyogenes* IdeS
176 (numbered from the start of the signal sequence) was sub-cloned into the expression vector
177 pET28b (Novagen). The coding sequencing was sub-cloned at the 3' end of Thioredoxin 6xHis-
178 TEV. The complete construct was sub-cloned as previously described (45) and was kindly
179 donated by Dr. Ulrich von Pawel-Rammingen from the Department of Molecular Biology, Umea
180 University. The transformation of pET-TRX_b plasmid harboring the IdeS encoding gene (pET-
181 IdeS) was carried out as follows: 200 μ l of chemical-competent *E. coli* BL21-DE3 cells were
182 thawed on ice for 20 minutes. 50ng of the plasmid pET-IdeS was added to the thawed competent
183 cells and incubated on ice for 20 minutes with gentle mixing every 5 minutes. Next, heat shock
184 was applied by incubating the cells at 42°C for 2 minutes followed by incubation on ice water for
185 2 minutes. For phenotypic expression, 800 μ l of LB was added, and cells were incubated at 37°C,
186 250 RPM for 1 hour in a horizontal position. Cells were plated on LB agar supplemented with
187 Kanamycin and incubated at 37°C overnight (O.N). Single colony was inoculated into 2ml LB
188 supplemented with Kanamycin and incubated O.N. at 37°C, 250 RPM. Next day, 2ml from the
189 grown cultures were inoculated into two 2liter flasks, each containing each 500ml LB
190 supplemented with Kanamycin. Over expression and purification of IdeS was carried out as
191 described for rhTNF α with a minor modification as follow: Ides was eluted with imidazole
192 gradient (50, 150, 500mM imidazole), total of 20ml. 20 fractions of 1ml were collected from each
193 elution step and evaluated for their purity using 12% SDS–PAGE. All fractions containing clean
194 IdeS were merged and dialyzed O.N. at 4°C against 4L of PBS (pH 7.4), using SnakeSkin dialysis
195 tubing with 10 kDa cutoff (Thermo Fisher Scientific). Dialysis products were analyzed by 12%
196 SDS–PAGE.

197

198

199 **Production of mAb-F(ab')₂**

200 Intact clinical grade IFX or ADL (designated here as mAb) were digested using in-house
201 produced IdeS. 10mg of mAb was incubated with 300µg of IdeS in the final volume of 500µl
202 PBS for 2.5 hours at 37^oC, followed by a spike-in of additional 300µg of IdeS to achieve full
203 digestion of the Fc fragments. IdeS inactivation was carried out by adding 0.1M of citric acid pH
204 3 and incubation for 1 minute at RT followed by the addition of PBS (pH 7.4) to neutralized
205 acidic pH. Next, reaction mixture was applied to a 1 mL HiTrap KappaSelect affinity column (GE
206 Healthcare Life Sciences). All affinity purification steps were carried out by connecting the
207 affinity column to a peristaltic pump with flow rate of 1ml/min. The reaction mixture was
208 recycled three times through the KappaSelect column to maximize the capture of intact mAb and
209 mAb-F(ab')₂. KappaSelect column was subsequently washed with 5CV of PBS and eluted with
210 10CV of 100mM glycine-HCl (pH 2.7). Collected 1ml elution fractions were immediately
211 neutralized with 100µl of 1.5M Tris-HCl (pH 8.8). Next, the recovered intact mAb and mAb-
212 F(ab')₂ fragments were applied to a custom packed 1ml Protein-G agarose column (GenScript).
213 The reaction mixture was recycled three times through the column, which was subsequently
214 washed with 5CV of PBS and eluted with 10CV of 100mM glycine-HCl (pH 2.7). The 10ml
215 elution fraction was immediately neutralized with 1ml of 1.5M Tris-HCl (pH 8.8). The recovered
216 10ml mAb-F(ab')₂ fragments were dialyzed overnight at 4°C against 4L of PBS (pH 7.4) using
217 SnakeSkin dialysis tubing with 10kDa cutoff (Thermo Fisher Scientific). Recovered mAb-F(ab')₂
218 sample were evaluated for purity by SDS-PAGE and their concentration measured by Take5
219 (BioTek instruments).

220 To test the functionality of the produced mAb-F(ab')₂, 96 ELISA plates (Nunc MaxiSorp™ flat-
221 bottom, Thermo Fisher Scientific) were coated with 1µg/ml of rhTNFα in PBS and incubated at
222 4°C O.N. ELISA plates were then washed three times with PBST and blocked with 300µl of 2%
223 w/v BSA in PBS for 1 hour at 37^oC. Next, 50nM of intact mAb and mAb-F(ab')₂ (IFX or ADL)
224 in blocking solution was added to each well in triplicates in a 3 fold dilution series, and plates
225 were incubated at RT for 1 hour. Next, plates were washed three times with PBST with 30 second
226 incubation time at each washing cycle. For detection, HRP conjugated anti-human kappa light
227 chain (Jackson) was added to each well (50µl, 1:5000 ratio in 2% w/v BSA in PBS) and incubated

228 for 1 hour at RT, followed by three washing cycles with PBST. Developing was carried out by
229 adding 50µl of TMB and reaction was quenched by adding 0.1M sulfuric acid. Plates were read
230 using the Epoch Microplate Spectrophotometer ELISA plate reader. To evaluate the purity of the
231 mAb-Fa(b')₂ samples (i.e. to make sure there are no traces of intact antibody or Fc fragment in the
232 sample), 96 ELISA plate (Nunc MaxiSorp™ flat-bottom, Thermo Fisher Scientific) were coated
233 with 5µg/ml of intact mAb and mAb-F(ab')₂ in PBS and incubated at 4°C O.N. Next, plates were
234 washed three times with PBST and blocked with 300µl 2% w/v BSA in PBS for 1 hour at 37°C.
235 Next, plates were washed three times with 300 µl PBST, followed by the incubation with HRP
236 conjugated anti-human IgG Fc antibody (Jackson) diluted 1:5000 in PBST. Developing was
237 carried out by adding 50µl of TMB and reaction was quenched by adding 0.1M sulfuric acid.
238 Plates were read using the Epoch Microplate Spectrophotometer ELISA plate reader (BioTek
239 Instruments).

240 **Generation of ADA standard**

241 A pool of 17 ADA to IFX positive sera were collected at Sheba Medical Center, and passed
242 through a 2ml custom packed protein G agarose column (GenScript). The pooled sera was
243 recycled three times over the column, which was subsequently washed with 5CV of PBS and
244 eluted with 10CV of 100mM glycine-HCl (pH 2.7). The 10ml elution fraction was immediately
245 neutralized with 1ml of 1.5M Tris-HCl (pH 8.8). The purified mAbs were immediately passed
246 over a custom made rhTNFα affinity column (NHS-activated agarose beads, Thermo Fisher
247 Scientific) in gravity mode. The purified mAbs were recycled three times over the column, which
248 was subsequently washed with 5CV of PBS and eluted with 10CV of 100mM glycine-HCl (pH
249 2.7). The 10ml elution fraction was immediately neutralized with 1ml of 1.5M Tris-HCl (pH 8.8).
250 The purified mAbs were dialyzed overnight at 4°C against 4L of PBS (pH 7.4) using SnakeSkin
251 dialysis tubing with 10kDa cutoff (Thermo Fisher Scientific). Purified mAbs were analyzed for
252 purity using 12% SDS-PAGE and concentration was determined by Take3 (BioTek instruments).

253 To test functionality, 96 ELISA plate were coated with 5µg/ml of mAb-F(ab')₂ in PBS (pH 7.4)
254 and incubated at 4°C O.N. ELISA plates were then washed three times with PBST and blocked
255 with 300µl of 2% w/v BSA in PBS for 1 hour at 37°C. Next, 50nM of the purified ADA in
256 blocking solution were added to each well in triplicates with 3-fold dilution series and plates were
257 incubated at RT for 1 hour. Next, plates were washed three times with PBST with 30 second
258 incubation time at each washing cycle. Next, anti-human Fc HRP conjugate (Jackson) was added
259 to each well at the detection phase (50µl, 1:5000 ratio in 2% w/v BSA in PBS) and incubated for

260 1 hour at RT, followed by three washing cycles with PBST. Developing was carried out by
261 adding 50µl of TMB and reaction was quenched by adding 0.1M sulfuric acid. Plates were read
262 using the Epoch Microplate Spectrophotometer ELISA plate reader.

263

264 **Quantitative measurement of ADA in serum**

265 The schematic configuration of the bio-immunoassay for the quantitative measurement of ADA in
266 serum is described in Fig. 3B and was carried out as follows: ELISA plates that were coated
267 overnight at 4°C with 5µg/ml produced IFX-F(ab')₂ in PBS (pH 7.4). ELISA plates were then
268 washed three times with PBST and blocked with 300µl of 2% w/v BSA in PBS for 1 hour at
269 37°C. Next, triplicates of 1:400 diluted serum samples were added at triplicates and serially
270 diluted 2 fold in 2% w/v BSA in PBS, 10% horse serum (Biological Industries) and 1% Tween 20
271 in PBS (1:400– 1:51,200 serum dilution factor). Plates were incubated for 1 hour at RT. On the
272 same plate, serial dilutions of 10nM ADA standard were incubated in triplicate and serially
273 diluted 2 fold in 2% w/v BSA in PBS, 10% horse serum (Biological Industries) and 1% Tween 20
274 in PBS, to allow the conversion of the tested serum to units per milliliter. ELISA plates were
275 washed three times with PBST and 50µl of HRP conjugated anti-human IgG Fc was added to
276 each well (50µl, 1:5000 ratio in 2% w/v BSA in PBS) and incubated for 1 hour at RT. ELISA
277 plate was then washed three times with PBST and developed by adding 50µl of TMB followed by
278 quenching with 50µl 0.1M sulfuric acid. Plates were read using the Epoch Microplate
279 Spectrophotometer ELISA plate reader.

280 **Neutralization index of ADA**

281 Neutralization capacity was determined using ELISA plates that were coated overnight at 4°C
282 with 5µg/ml IFX-F(ab')₂ in PBS (pH 7.4 ELISA plates were then washed three times with PBST
283 and blocked with 300µl of 2% w/v BSA in PBS for 1 hr at 37°C. Next, triplicates of 1:400 diluted
284 serum samples were added to the negative TNFα wells and serially diluted 2 fold in 2% w/v BSA
285 in PBS, 10% horse serum (Biological Industries) and 1% Tween 20 in PBS. Triplicates of 1:400
286 diluted serum samples with 200nM rhTNFα were also added to the remaining wells and serially
287 diluted 2 fold in 2% w/v BSA in PBS, 10% horse serum (Biological Industries) and 1% Tween 20
288 in PBS (1:400– 1:51,200 serum dilution factor). Plates were incubated for 1 hour at RT. ELISA
289 plates were washed three times with PBST and 50µl of HRP conjugated anti-human IgG Fc

290 antibody or anti HRP conjugated His-tag antibody were added at the detection phase (50µl,
291 1:5000 ratio in 2% w/v BSA in PBS) and incubated for 1 hour at RT, followed by three washing
292 cycles with PBST. Developing was carried out by adding 50µl of TMB and reaction was
293 quenched by adding 0.1M sulfuric acid. Plates were read using the Epoch Microplate
294 Spectrophotometer ELISA plate reader. Neutralization index was calculated by the logarithmic
295 score of triplicate average differences between the ELISA equation curve without rhTNFα and in
296 the presence of rhTNFα where the value of the control background is above 3-x standard
297 deviation.

298 **Blood processing**

299 IFX treated patients with IBD cared for in the Department of Gastroenterology at the Sheba
300 medical center were included in the study. All subjects signed an informed consent, and the study
301 was approved by the Ethics Committee of the medical center. All patients received IFX on a
302 scheduled regimen and blood samples were drawn immediately before their scheduled IFX
303 infusion. Blood was collected into a single Vacutainer Lithium Heparin collection tube (BD
304 Bioscience).

305 For NGS analysis, blood was collected from a male donor treated with IFX, before IFX
306 administration and 10 days after administration. 30ml of peripheral blood were collected into 3
307 single Vacutainer K-EDTA collection tubes (BD Biosciences). Collection of peripheral blood
308 mono-nuclear cells (PBMCs) was performed by density gradient centrifugation, using Uni-
309 SepMAXI+ lymphocyte separation tubes (Novamed) according to the manufacturer's protocol.

310 **Fluorescence-Activated Cell Sorting Analysis and sorting of B cell populations**

311 PBMCs were stained for 15 minutes in cell staining buffer (BioLegend) at RT in the dark using
312 the following antibodies: anti-CD3–PerCP (clone OKT3; BioLegend), anti-CD19– Brilliant
313 Violet 510 (clone HIB19; BioLegend), anti-CD27–APC (clone O323; BioLegend), anti-CD38–
314 APC-Cy7 (clone HB-7; BioLegend), and anti-CD20–FITC (clone 2H7; BioLegend).

315 The following B cell population was sorted using a FACS Aria cell sorter (BD Bioscience):
316 CD3–CD19+CD20–CD27++CD38^{high}

317 B cell subpopulations were sorted and collected into TRI Reagent solution (Sigma Aldrich) and
318 frozen at –80°C.

319 **Amplification of V_H and V_L repertoires from B cells**

320 Total RNA was isolated using RNeasy micro Kit (Qiagen), according to manufacturer's protocol.
321 First-strand cDNA generation was performed with 100ng of isolated total RNA using a
322 SuperScript RT II kit (Invitrogen) and oligo-dT primer, according to manufacturer's protocol.
323 After cDNA synthesis, PCR amplification was performed to amplify the V_H and V_L genes using a
324 primer set described previously (25) with overhang nucleotides to facilitate Illumina adaptor
325 addition during the second PCR (Table S1). PCR reactions were carried out using FastStart™
326 High Fidelity PCR System (Roche) with the following cycling conditions: 95°C denaturation for
327 3 min; 95°C for 30 sec, 50°C for 30 sec, and 68°C for 1 min for four cycles; 95°C for 30 sec,
328 55°C for 30 sec, and 68°C for 1 min for four cycles; 95°C for 30 sec, 63°C for 30 sec, and 68°C
329 for 1 min for 20 cycles; and a final extension at 68°C for 7 min. PCR products were purified using
330 AMPure XP beads (Beckman Coulter), according to manufacturer's protocol (ratio x 1.8 in favor
331 of the beads). Recovered DNA products from the first PCR was applied to a second PCR
332 amplification to attach Illumina adaptors to the amplified V_H and V_L genes using the primer
333 extension method as described previously (31). PCR reactions were carried out using FastStart™
334 High Fidelity PCR System (Roche) with the following cycling conditions: 95°C denaturation for
335 3 min; 95°C for 30 sec, 40°C for 30 sec, and 68°C for 1 min for two cycles; 95°C for 30 sec, 65°C
336 for 30 sec, and 68°C for 1 min for 7 cycles; and a final extension at 68°C for 7 min. PCR products
337 were applied to 1% agarose DNA gel electrophoresis and gel-purified with Zymoclean™ Gel
338 DNA Recovery Kit (Zymo Research) according to the manufacturer's instructions. V_H and V_L
339 libraries concentration were measured using Qubit system (Thermo Fisher Scientific) and library
340 quality was assessed using the Bioanalyzer 2100 system (Agilent) or the 4200 TapeStation system
341 (Agilent). All V_H libraries were produced in duplicates starting with RNA as the common source
342 template. The V_L were produced with one replicate.

343 V_H and V_L libraries from sorted B cell were subjected to NGS on the MiSeq platform with the
344 reagent kit V3 2x300 bp paired-end (Illumina), using an input concentration of 16pM with 5%
345 PhiX.

346 Raw fastq files were processed using our recently reported ASAP webserver (29). ASAP analysis
347 resulted in a unique, full-length V_H and V_L gene sequences database for each time point. The
348 resultant database was used as a reference database to search the LC-MS/MS spectra.

349 **Proteomic Analysis of the Serum ADA to IFX**

350 Total IgG from each time point (D0, D10) were purified from 7-10ml of serum by protein G
351 enrichment. Serum was diluted 2 fold and passed through a 5ml Protein G agarose column
352 (GeneScript). The diluted serum was recycled three times over the column, which was
353 subsequently washed with 10CV of PBS and eluted with 7CV of 100mM glycine-HCl (pH 2.7). A
354 total of 35 fractions of 1ml were collected and immediately neutralized with 100 μ l of 1.5M
355 Tris-HCl (pH 8.8). All elution fractions were evaluated for their purity using 12% SDS-PAGE
356 and 11 purified 1 ml IgG fractions were combined and dialyzed overnight at 4°C against 4L of
357 PBS (pH 7.4) using SnakeSkin dialysis tubing with 1 kDa cutoff (Thermo Fisher Scientific).

358 Next, 9mg of total IgG were digested with 100 μ g of IdeS in the final volume of 2ml PBS for 5
359 hour at 37°C. IdeS inactivation was carried out by adding 0.1M of citric acid pH 3 and incubation
360 for 1 minute at RT followed by the addition of PBS (pH 7.4) to neutralize the low pH. Total
361 serum F(ab')₂ was then applied to a one ml custom made affinity column comprised of IFX-
362 F(ab')₂ coupled to NHS-activated agarose beads (Thermo Fisher Scientific). The purified serum
363 F(ab')₂ were recycled three times over the affinity column, which was subsequently washed with
364 5CV of PBS and eluted with 15CV of 100mM glycine-HCl (pH 2.7) and collected into Maxymum
365 Recovery Eppendorf (Axygen Scientific). A total of 30x0.5ml elution fractions and 1x50ml flow-
366 through were immediately neutralized with 50 and 100 μ l (respectively) of 1.5M Tris-HCl (pH
367 8.8). The purified antigen-specific F(ab')₂ were dialyzed overnight at 4°C against 4L of PBS (pH
368 7.4) using SnakeSkin dialysis tubing with 10kDa cutoff (Thermo Fisher Scientific). Elution and
369 flow-through fractions were trypsin-digested, and resulting peptides were fractionated and
370 sequenced by nanoflow LC-electrospray MS/MS on an Orbitrap Velos Pro hybrid mass
371 spectrometer (Thermo Scientific), in the UT Austin mass spectrometry core facility as described
372 previously (38). MS/MS raw files were analyzed by MaxQuant software version 1.6.0.16 (46)
373 using the MaxLFQ algorithm (47) and peptide lists were searched against the common
374 contaminants database by the Andromeda search engine (48) and a custom protein sequence
375 database consisting of the donor-specific V_H and V_L sequences derived from NGS of individual
376 donor B cells. All searches were carried out with cysteine carbamidomethylation as a fixed
377 modification and methionine oxidations as variable modifications. The false discovery rate was
378 set to 0.01 for peptides with a minimum length of seven amino acids and was determined by
379 searching a reverse decoy database. Enzyme specificity was set as C-terminal to arginine and
380 lysine as expected using trypsin as protease, and a maximum of two missed cleavages were
381 allowed in the database search. Peptide identification was performed with an allowed initial
382 precursor mass deviation up to 7ppm and an allowed fragment mass deviation of 20ppm. For LFQ

383 quantification the minimal ratio count was set to 2, and match between runs was performed with
384 three mass-spec injections originating from the same sample. MaxQuant output analysis file,
385 “peptides.txt”, was used for further processing. Total peptides that were identified in the elution
386 samples were filtered using the following criteria: (a) were not identified as contaminants; (b) did
387 not match to the reversed decoy database; (c) were identified as peptides derived from the region
388 comprising the CDRH3, J region, FR4 and the ASTK motif (derived from the N-terminal of the
389 C_{H1} region). The CDRH3 derived peptides were further characterized as informative CDRH3
390 peptides (*i*CDRH3 peptides) only if they map exclusively to a single antibody clonotype. A
391 clonotype was defined as all sequences that comprise CDRH3 with the same length and identity
392 tolerating one amino acid mismatch, and same V, J family. The intensities of high confidence
393 *i*CDRH3 peptides were averaged between replicates while including only peptides that were
394 observed in at least two out of the three replicates. Clonotype frequencies within each sample
395 were calculated using only *i*CDRH3 peptides and were determined to be antigen-specific if their
396 frequency in the elution fraction was at least 5 fold greater than their frequency in the flow-
397 through fraction. The CDRH3 sequences identified by the mapping of high confidence MS/MS
398 peptides were used to generate a complete list of full length VH sequences. These VH sequences
399 were used to analyze the repertoire measures of the antibodies that were identified in the donors’
400 serum.

401 **Study population**

402 IFX and ADL treated patients with IBD cared for in the Departments of Gastroenterology at
403 Sheba medical center were included in the study. All subjects signed an informed consent, and the
404 study was approved by the Ethics Committee of Sheba medical center. IFX and ADL and ADA
405 serum levels were routinely measured at trough immediately before infusion. All patients received
406 IFX and ADL on a scheduled regimen. All patients that were included in this study exhibited low
407 through levels of IFX and ADL.

408 **Statistical analysis**

409 All curves were fitted on a sigmoidal dose–response curve and EC50 of each was calculated.
410 Mann-Whitney test was used to compare continuous variables. All reported P values were two-
411 tailed, and a P value less than 0.05 were considered statistically significant. All statistics were
412 performed with GraphPad Prism software (version 7, San Diego, California).

413 **Results**

414 **Production of mAb-F(ab')₂ to be used in the bio-immunoassay**

415 To investigate the molecular landscape of ADA following mAb administration we first aimed to
416 develop an accurate, sensitive, robust bio-immunoassay to determine ADA levels in sera. The
417 working hypothesis was that anti-idiotypic antibodies dominate the ADA compartment (21) thus,
418 the developed bio-immunoassay was based on the drugs' F(ab')₂ portion to be used as the antigen
419 (i.e. coating agent).

420 To achieve this, we used the immunoglobulin G (IgG)-cleaving enzyme (IdeS), a cysteine
421 proteinase enzyme that proteolytically cleaves immunoglobulins below the hinge region (22)
422 (Figure 1A). IFX was digested using IdeS by incubating 10 mg of clinical grade mAb with IdeS
423 to reach near complete digestion. Next, IFX-F(ab')₂ was purified from Fc regions and undigested
424 full IFX by consecutive affinity chromatography steps comprising protein A and kappaSelect
425 columns.

426 Recovered IFX-F(ab')₂ purity was evaluated by SDS-PAGE (Figure 1B) and ELISA (Figure 1C)
427 to ensure that the IFX-F(ab')₂ exhibits no traces of IFX-Fc/undigested IFX that will contribute to
428 the background level when using anti-Fc HRP conjugate at the detection phase. Recovered IFX-
429 F(ab')₂ samples were found to be highly pure with basal anti-Fc signal levels similar to the signal
430 observed in the control samples. The produced IFX-F(ab')₂ was tested for functionality by
431 measuring its TNF α binding capacity, using ELISA with TNF α as the coating agent, and was
432 found to show similar functionality as that of the intact IFX (Figure 1D). ADL was subjected to
433 the same preparative pipeline and demonstrated similar results (Figure S1).

434 **ADA Standard curve**

435 Quantification of total ADA in serum requires a standard reference. Thus, we generated a
436 standard ADA pool that facilitates the quantification of ADA levels in sera of patient treated with
437 IFX. ADA were pooled from several serum samples collected from patients treated with IFX and
438 purified by consecutive affinity chromatography steps comprising protein G and a custom-made
439 IFX-F(ab')₂ affinity columns. We confirmed the affinity enrichment of ADA by applying the
440 affinity chromatography elution fraction to ELISA with IFX-F(ab')₂ as the coated antigen (Figure
441 2A). The purity and concentration the recovered ADA were determined by SDS-PAGE (Figure
442 2B) and nanodrop.

443 Maximal serum concentration used in a bio-immunoassay (e.g. serum diluted 1:100 or 1:200) is a
444 major factor that may contribute to high background signal levels due to non-specific binding.
445 Screening several maximal serum dilutions showed that 1:400 initial serum dilution demonstrates
446 the lowest background signal (data not shown). To evaluate if serum will affect the signal
447 obtained from purified ADA, we spiked-in purified ADA into negative control serum that was
448 diluted 1:400 in PBS. Serial dilution of spiked-in ADA and purified ADA showed similar signal
449 in ELISA (Figure 2C) indicating that serum does not bias the ADA detection in our developed
450 bio-immunoassay.

451 **Quantitative measurement of ADA in serum**

452 ADA detection is technically challenging as both the analyte and antigen are antibodies which
453 may result in the inability to differentiate between the mAb and ADA. To overcome this
454 challenge, many assays were previously developed (5). One of these immunoassays is the anti-
455 human λ chain (AHLC) immunoassay that is used in clinical setups for monitoring the formation
456 of ADA (23). The principle of this assay is to detect ADA comprising λ light chain, thus avoiding
457 cross reactivity with the drug that comprises the κ light chain (Figure 3A).

458 While AHLC is suitable for monitoring the development of ADA in clinical setups, when one
459 aims to study the molecular composition of ADA there is a need to provide quantitative measures
460 of total ADA in serum. Thus, we developed a new bio-immunoassay based on the $F(ab')_2$ portion
461 of the mAb. The bio-immunoassay setup is described in Figure 3B and is based on mAb- $F(ab')_2$
462 as the coating antigen and anti-Fc HRP conjugate used as the detection antibody. Each of the
463 experimental setups to test ADA in serum included serum from a healthy donor as a control and
464 ADA standard for the quantitation of total ADA.

465 First, we applied the newly developed bio-immunoassay on two serum sample groups: one
466 negative and one positive for ADA as determined by the AHLC assay (AHLC⁽⁻⁾ and AHLC⁽⁺⁾,
467 respectively). We also included serum from a healthy subject to serve as a control for the assay
468 specificity (i.e. serum from a subject that was not exposed to IFX). As shown in Figure 3C-D, the
469 ELISA signals obtained when utilizing the new bio-immunoassay were higher compared to the
470 signal obtained with the AHLC assay. Moreover, applying the new bio-immunoassay on the
471 AHLC⁽⁻⁾ serum (no detected ADA with the AHLC assay) detected relatively high levels of ADA.
472 These results indicate that not all ADA were detected with the AHLC assay as this assay is based
473 on the detection of ADA that comprise the λ light chain only.

474 Next, to extend and generalize the above results, sera from 55 patients treated with IFX were
475 collected at the Chaim Sheba Medical Center and tested for drug levels and ADA using the
476 AHLC assay. The established cohort showed very low drug trough levels and based on the AHLC
477 results, sera were stratified into two groups: 26 serum samples were identified as AHLC⁽⁻⁾ and 29
478 as AHLC⁽⁺⁾. Using our newly developed quantitative bio-immunoassay, we found that ADA
479 levels in tested sera ranged between 2.7 to 1268.5 µg/ml. Serum ADA levels using AHLC
480 compared to the new bio-immunoassay are summarized in Table 1. More importantly, the new
481 bio-immunoassay demonstrated improved sensitivity compared to AHLC assay manifested in the
482 detection of higher concentrations of ADA in 40 out of the 55 serum samples, of which 12 out of
483 the 55 samples, belong to the AHLC⁽⁻⁾ group. Overall, the average fold increase in ADA detection
484 using the new bio-immunoassay compared to the AHLC assay was 17.3 and 60.6 for the AHLC⁽⁺⁾
485 and AHLC⁽⁻⁾ groups , respectively.

486 **Neutralization index of ADA**

487 Due to high clinical relevance and different mechanism of action of *bADA* and *ntADA*,
488 identifying their relative abundances in serum can provide valuable insights regarding the nature
489 of the immune response following mAb administration. We therefore modified our newly
490 developed mAb-F(ab')₂ based bio-immunoassay by blocking the coated IFX-F(ab')₂ binding site
491 with TNFα in order to obtain a differential signal compared to the unblocked assay (Figure 4A).
492 In order to block the binding site of IFX-F(ab')₂ towards TNFα and prevent the binding of anti-
493 idiotypic ADA (i.e. *ntADA*) to the drug, recombinant human TNFα (rhTNFα) fused to a His-tag
494 was cloned and expressed (see materials and methods). In-house production of rhTNFα was
495 essential, as the N terminal His-tag was used for monitoring the presence of the rhTNFα
496 throughout the bio-immunoassay.

497 First, we evaluated the ability of rhTNFα to inhibit the binding of ADA to the coated IFX-F(ab')₂
498 by setting up a competitive ELISA where a series of ADA standard concentrations were
499 incubated with a series of fixed rhTNFα concentrations (data no shown). We observed a
500 competitive effect while rhTNFα was fixed at the concentration of 5nM (Figure 4B). This step
501 was important as it enabled us to determine the ADA equimolar concentration of rhTNFα to be
502 used that will fully occupy the IFX-F(ab')₂ binding site and will prevent the binding of *ntADA* to
503 the coated (and blocked) IFX-F(ab')₂. We monitored the presence of rhTNFα using an HRP-
504 conjugated anti-His tag antibody and observed that if we aim to completely block ADA it is

505 required to use equimolar concentration of rhTNF α that corresponds to the highest
506 concentration of ADA in the assay (200nm).

507 In practice, IFX-F(ab')₂ binding site was blocked with rhTNF α by prior incubation of serum with
508 the coated IFX-F(ab')₂ hence, the differential signal w/ and w/o the presence of rhTNF α represent
509 the portion of ADA that could not bind the IFX-F(ab')₂ binding site thus, reflects the
510 neutralization capacity (hereby named neutralization index) of the ADA in the tested serum.
511 Using this assay, we evaluated the neutralization index of the 55 sera from patients treated with
512 IFX and 7 sera from patients treated with ADL. In sera from patients treated with IFX, we noticed
513 that there are two main neutralization index patterns: those with high differential signal (Figure
514 5A) and low differential signal (Figure 5B). More interestingly, we found that patients that were
515 stratified as AHLC⁽⁺⁾ have a significantly higher neutralization index compared to those that
516 belong to the AHLC⁽⁻⁾ group (Figure 5C). This suggests that there is a preferential usage of the
517 λ light chain in ntADA as the AHLC⁽⁺⁾ group is *a priori* defined by the presence of ADA
518 comprising the λ light chains. All sera from patients treated with ADL (n=7) were subjected to
519 modified bio-immunoassay and demonstrated high neutralization indexes (Figure S2)

520

521 **IFX infusion induces a vaccine like immune response**

522 To further investigate the molecular landscape of ADA we explored the dynamics of the B cell
523 response following mAb administration. When investigating well-controlled clinical scenarios
524 such as samples obtained from post-vaccinated individuals, it is convenient to isolate the antigen-
525 specific B cell as they peak at a defined time window (24, 25). However, the characteristics of the
526 humoral response and ADA encoding B cell dynamics following mAb administration is unknown.
527 Our working hypothesis assumed that the immune response following mAb administration is a
528 vaccine-like response thus; we expected to observe a wave of PB peaking several days after IFX
529 infusion. It was previously demonstrated that boost vaccines induce a strong proliferation of PBs
530 and mBCs that can be detected in the blood circulation several days after the boost (26, 27). To
531 test if IFX administration induces a vaccine like response, we collected blood samples from a
532 patient that was found to be positive to ADA at two time points: prior to IFX infusion (D0) and 10
533 days after IFX infusion (D10). The second time point (D10) was determined in order to capture an
534 enriched population of antigen-specific PB as well as mBC that enable the establishment of a
535 donor-specific V_H database for the proteomic interpretation of peptides derived from ADA.

536 Peripheral blood mononuclear cells (PBMCs) were sorted by FACS and the frequency of PB
537 (CD3⁻CD19⁺CD20⁻CD27⁺⁺CD38⁺⁺) and mBC (CD3⁻CD19⁺CD20⁺CD27⁺) subsets were
538 determined. We identified a 13-fold increase in the frequency of PB at D10 and no increase in the
539 mBC compartment. The PB data suggests that the B cell dynamics following IFX infusion
540 exhibits vaccine-like characteristics in accordance with our working hypothesis (Table 2, Figure
541 S3).

542 **Antibody repertoire of ADA encoding B-Cells**

543 The waves of PB following challenge is enriched with antigen-specific B cells (24, 25, 28). Based
544 on this, a major fraction of PB at D10 post mAb infusion is expected to comprise B cell clones
545 responding to the current antigen challenge. Thus, the repertoire of B cells at two time points
546 (pre- and post-infusion) is predicted to represent the overall differences in the ongoing ADA
547 encoding B cell response.

548 This diversity of antibodies is accomplished by several unique molecular mechanisms, including
549 chromosomal V(D)J rearrangement, somatic hypermutations (SHM) and class switch
550 recombination (29), processes that are mediated by recombination-activating gene (RAG) and
551 activation-induced cytidine deaminase (AID), respectively. The AID enzyme functions mainly in
552 secondary lymph nodes named germinal centers. Next-generation sequencing (NGS) of the
553 antibody variable regions (V-genes) coupled with advanced bioinformatics tools provides the
554 means to elucidate the antigen-specific antibody repertoire's immense diversity (30). To deep
555 sequence antibodies' V-genes, recovered RNA from sorted PB and mBC was used as the
556 template for first-strand cDNA synthesis, followed by PCR amplification steps to produce
557 barcoded amplicons of the V-genes of the antibody heavy chains (V_H) as described previously
558 (31). While NGS of antibodies is a powerful tool for immune repertoire analysis, relatively high
559 rates of errors accumulate during the experimental procedure. To overcome this challenge, we
560 generated duplicates of the antibody V-gene amplicons and sequenced them using the Illumina
561 MiSeq platform (2x300bp). The resultant V_H sequences were processed using our recently
562 reported ASAP webserver that was specifically developed to analyze NGS of antibody V-gene
563 sequences derived from replicates (29).

564 In our analysis, we concentrated on several repertoire measures that collectively provide a
565 molecular level characterization of the ADA: i) V(D)J family usage; ii) CDR3 length distribution;
566 iii) SHM levels, and, iv) isotype distribution. Our data revealed several interesting antibody

567 repertoire features that may shed light on the molecular mechanism involved in the formation of
568 ADA.

569 V(D)J gene family usage is stable

570 Examining the V(D)J family usage is important to determine whether the basal gene frequency is
571 similar to the expected frequency and if the B cell response following IFX infusion drives B cells
572 to exhibit a preferential V(D)J gene usage. Therefore, we examined the frequency of family usage
573 at two time points (D0 and D10), within PB and mBC subsets across isotypes (IgG and IgM).
574 The V(D)J family usage showed no marked difference between the two time points, B cell subsets
575 and isotypes. The frequency of V-gene family usage was also found to have similar frequency
576 profile as previously described (32, 33). For example, the V-gene family frequency showed that
577 the V3, V4 and V1 have the most prevalent representation followed by V2, V5 and V6 that had
578 significantly lower frequencies (Figure 6A). The same pattern trends were identified for the D and
579 J family usage.

580 CDRH3 length increases following IFX infusion

581 Composed of the V(D)J join with its inherent junctional diversity, the CDRH3 specifies the
582 antibody V_H clonotype. The V_H clonotype is an important immunological concept because it
583 accounts for antibodies that likely originate from a single B-cell lineage and may provide insight
584 on the evolution of the antigen-specific response (34). Here we defined V_H clonotype as the group
585 of V_H sequences that share germ-line V and J segments and have identical CDRH3 sequences. By
586 examining the length distribution of CDRH3 from PB across isotypes and time point we observed
587 a shift towards longer CDRH3 at D10 (Figure 7). Interestingly, this observation is in contrast to
588 previous studies that reported a decrease in the CDRH3 length post immunization with
589 pneumococcal (35) and hepatitis B vaccines (36) and when comparing antigen experienced B cell
590 to naïve B cells (37).

591 Somatic hypermutation levels decreases following IFX infusion

592 Examining the level of SHM following vaccination provides insights regarding the extent of the
593 affinity maturation that antigen-stimulated B cell undergo. It was previously reported that boost
594 vaccination induces a substantial increase of the SHM levels when comparing post- to pre-
595 vaccination (36). Despite the vaccine like response following IFX infusion, we observed in the

596 PB compartment a significant decrease in the SHM levels post-infusion, regardless if the
597 mutations were synonymous and non-synonymous (Figure 8).

598 **Proteomic analysis of ADA**

599 Analysis of serum antibodies provides a comprehensive profile of the humoral immune response
600 and is complementary to the transcriptomic analysis derived from NGS of the antibody V_H.
601 Applying an approach that integrates NGS and tandem mass spectrometry (LC-MS/MS) has been
602 shown to provide valuable data regarding the composition of antigen-specific serum antibodies
603 and their relationship to B cells and generates new insights regarding the development of the
604 humoral immune response in disease and following vaccination (24, 25). Here we utilized the
605 previously developed omics approach (34, 38) to elucidate the serum ADA composition following
606 IFX infusion. ADA from 10 ml of serum collected at D0 and D10 were subjected to protein G
607 affinity chromatography and total of 9 mg of recovered IgG was digested by IdeS to remove the
608 Fc regions that may mask the MS/MS signal obtained from low abundant peptides. Following 5
609 hours of digestion, the reaction mixture was subjected to custom made affinity column where the
610 IFX-F(ab')₂ was coupled to agarose beads and served as the antigen to isolate ADA. Recovered
611 48.57µg polyclonal ADA-F(ab')₂ (i.e., IFX-F(ab')₂-specific IgG's) in the elution fraction and
612 total F(ab')₂ (depleted from ADA-F(ab')₂) in the flow through fraction were digested with trypsin
613 and injected to high-resolution tandem mass spectrometer analyzer in triplicates. LC-MS/MS raw
614 data files were analyzed using MaxQuant using label free quantitation mode (LFQ) and searched
615 against the custom antibody V-gene database derived from the NGS data of B cells isolated from
616 the same donor. Identified peptide from the interpretation of the proteomic spectra were stratified
617 into three types of peptides: informative peptides (*i*Peptide) that map uniquely to one antibody
618 clonotype in a region that is upstream to the CDRH3, non-informative CDRH3 peptides
619 (*ni*CDRH3) that map to the CDRH3 region of the antibody but do not map uniquely to a single
620 antibody clonotype and informative CDRH3 peptides (*i*CDRH3) that map uniquely to a single
621 antibody clonotype. Summary of identified peptides in LC-MS/MS are shown in Table 3. Beyond
622 the designation as *i*CDRH3 peptides, additional filtration steps were applied including peptides
623 that were present in more than 2 replicates, peptides in elution that show 5x fold frequency than in
624 the flow through. The *i*CDRH3 peptides enabled the identification of 62 unique ADA CDRH3
625 clonotypes with 205 associated full-length V-gene sequences. The resulting V-gene sequences
626 were analyzed to determine their V(D)J family usage and the B cell subset they are mapped to,
627 based on our NGS data (Figure 9).

528 The V(D)J family usage of the antibody variable region sequences that were identified by LC-
529 MS/MS (Figure 9A) showed a similar distribution as observed in the NGS data (Fig. 6A, Fig.
530 7A). V family frequency analysis showed that the V1, V3, and V4 are the most dominant V
531 families followed by V2 and V5 that had significantly lower frequencies. D family frequency
532 analysis showed that the D6, D3, D2 and D1 have the most prevalent representation, and J family
533 frequency showed that the J4, J5 and J6 have the most prevalent representation.

534 Next, we examined the distribution of the proteomically identified V-gene sequences to B cell
535 subsets (Figure 9B) and found that the V-genes predominantly map to mBC from D0 (46.83%),
536 followed by mBC from D10 (27.8%). Moreover, we found that 23.9% of V-genes map to D10
537 PB. Based on the dynamics of antibodies in serum (24), the majority of antibodies produced
538 following a boost challenge are the product of pre-existing mBC cells that were re-activated
539 following drug infusion, much like a response to a vaccine boost (25).

540 As mentioned above, flow cytometry of B cells following IFX administration allowed us to
541 identify a substantial increase in the frequency of PB at D10, which suggests that the B cell
542 dynamics following IFX infusion exhibits vaccine-like characteristics. Therefore, we expected to
543 find a majority of V-gene sequences mapping to IgG⁺ B cells that underwent class switch
544 recombination in the germinal center. Surprisingly, the majority of proteomically identified serum
545 antibodies were mapped to IgM⁺ B cells (Figure 9C).

546 Next, we aimed to provide support to the observation that *ntADA* preferably use the λ light chain.
547 By quantifying the accumulative intensities of peptides derived from the constant region of both
548 light chains we calculate the change in the ratio between peptide that were derived from the
549 affinity chromatography elution fraction (ADA) and the flow through fraction (non-ADA). The
550 expected κ/λ ratio of total IgG in serum is 2 (66% κ and 33% λ). Indeed, proteomic analysis of
551 the affinity chromatography flow through fractions (D0 and D10) that represent the total IgG
552 population depleted from ADA, resulted in average κ/λ ratio of 2.1. The same analysis of the
553 elution fraction showed a significant shift of the κ/λ ratio to 1.19. These data support our
554 serological data that *ntADA* preferably use the λ light chain and thus, contribute to the shift in the
555 κ/λ ratio.

556 Discussion

557 The use of therapeutic mAbs in treating a wide range of diseases and disorders is growing
558 exponentially. Nonetheless, a major shortcoming of their use is the development of ADA in
559 patients receiving the mAb. Advances in mAb engineering have enabled the development of fully
560 human mAbs with reduced immunogenicity without abolishing it completely. Thus a mAb
561 administered to a patient can still induce an immune sensitization as reflected by the production of
562 ADA, which is associated with low trough drug levels and can mediate loss of clinical response to
563 the drug (20).

564 The precise mechanism underlying ADA production is unknown, and many questions related to
565 its development remain unaddressed, including determining precise concentrations of ADA in
566 serum, which portion of the ADA exhibits neutralizing capacity, the immune pathway governing
567 the production of ADA, and ultimately, the molecular composition of ADA at the sequence level.
568 To address these questions, we chose the chimeric TNF α antagonist IFX as the model system.
569 First, we aimed to quantify the ADA level in patient sera. Many methods were previously
570 reported to evaluate serum ADA levels; however, those assays provide mostly qualitative
571 measures to assist physicians in deciding the most appropriate intervention when treating patients,
572 and many (if not all) studies underestimated actual ADA levels (19). To provide quantitative
573 measures describing the molecular landscape of ADA, we first developed a bio-immunoassay that
574 would allow quantify ADA levels based on the F(ab')₂ region of the mAb because previous
575 reports indicated that the ADA generated from mAb administration are mostly anti-idiotypic (21).
576 Indeed, the bio-immunoassay demonstrated higher sensitivity compared with the AHLC assay
577 used initially to detect ADA and was able to detect ADA when the AHLC assay could not.
578 Leveraging its improved sensitivity, we applied our proprietary assay on sera from 55 patients
579 treated with IFX and found that patients designated as AHLC⁽⁺⁾ showed significantly higher levels
580 of ADA (mean: 264 μ g/ml) compared to the AHLC⁽⁻⁾ group (mean: 57 μ g/ml). These results
581 support the clinical use of AHLC assay because overall, patients were correctly stratified leading
582 to clinical decision-making that was based on a valid indicative assay. Notwithstanding, the
583 applicability of the AHLC assay, the newly developed F(ab')₂-based bio-immunoassay
584 demonstrated that ADA levels can reach extreme concentrations that were not detected using the
585 AHLC assay.

586 Some patients who develop ADA in response to IFX present a prolonged remission with
587 maintenance therapy despite repeated indications of high ADA and low IFX trough levels (20).
588 The mechanism of action of these ADA has significant influence on drug efficacy. For example,

589 *b*ADA are most likely to enhance the clearance of a drug whereas *nt*ADA will prevent a drug
590 from binding to its target. Hence, it is important to differentiate between *b*ADA and *nt*ADA, or in
591 other words, a need exists to identify sera with high levels of *nt*ADA that may predict the
592 likelihood of a patient losing a favorable response to an administered mAb. To achieve this, we
593 further revised our bio-immunoassay to qualitatively measure the neutralization index of ADA in
594 the serum of patients treated with IFX. Using this assay on sera from the 55 patients, revealed that
595 patients who tested positive utilizing the AHLC assay, exhibit a significantly higher neutralization
596 index than patients tested negatively for it (i.e., AHLC⁽⁻⁾). Noteworthy, the AHLC assay is based
597 on the anti- λ light chain antibody at the detection stage, suggesting that ADA with high
598 neutralization index preferably use the λ light chain. This phenomenon received additional
599 support from our proteomic analysis in which we compared the changes in the ratio between
700 peptides derived from κ and λ constant light chains from IFX-specific IgG pool and peptide
701 derived from total IgG polyclonal pool. This analysis demonstrated that the κ/λ ratio in the total
702 IgG compartment is as expected and is decreased in the mAb-specific compartment (κ/λ ratio 2.1
703 and 1.19 for total IgG and ADA, respectively). The preferential use of the λ light chain in
704 neutralizing antibodies has been previously reported (21, 39), however, the authors of those
705 studies did not provide an explanation beyond the structural adaptability of the light chain toward
706 the target. The relevance of the reported cases showing λ chain bias is not clear. Similar
707 phenomena was reported in B-1 sub-population, unlike follicular B cells, B-1 cells exhibit an
708 increased frequency of lambda light chains (40). The recurrence of BCRs with the enrichment of
709 λ light chain has been considered to result from strong antigen-dependent selection of the B-1 cell
710 repertoire (41).

711 Repetitive administration of mAbs may induce a strong humoral response manifested in the
712 production of ADA. We hypothesized that mAb administration is similar to the response that
713 occurs following a boost vaccine. Others and we have demonstrated that boost vaccines induce a
714 strong proliferation of PB that can be detected in blood circulation several days after the boost.
715 The “wave” of B cells after the boost vaccine are dominated by antigen-specific B cell (27) thus,
716 repertoire analysis of these cells can provide invaluable data about the antigen-specific antibody
717 repertoires. Utilizing flow cytometry showed an order of magnitude increase in PB compartment
718 10 days after IFX infusion, suggesting that the immune response following IFX administration is
719 indeed similar to a vaccine response. To the best of our knowledge, this is the first report to
720 identify a vaccine like response following therapeutic mAb administration.

721 Next, we aimed to provide a comprehensive repertoire profile of the B cells induced after mAb
722 administration. To achieve this, we applied an “omics” approach as previously described (25, 34,
723 38) that is based on the integration of NGS of the V-genes and proteomic analysis of serum ADA.
724 NGS of V-genes revealed no bias in the V(D)J usage across isotypes, cell types, and time point.
725 These data suggest that the original repertoire that existed before mAb administration and
726 antigen-specific repertoire induced by IFX administration is formed by random recombination
727 processes without preferential use of any particular V(D)J segment. Comparative repertoire
728 analysis of the V-genes between time points (before and after IFX administration) revealed that
729 post-IFX administration, PB exhibit longer CDRH3 and lower SHM rates. Although the B cell
730 dynamics after mAb administration are similar to those that occur after a boost vaccine, the
731 repertoire measures show a different profile. It was previously reported that the antibodies
732 generated after a boost vaccine exhibit shorter CDRH3, high SHM (35-37).

733 To explain these data we revisited two reports: the first describes how the immune response in
734 TNF α -deficient mice was “diverted” to the marginal zone instead of to the germinal center (42)
735 and the characteristics of the immune response in the marginal zone is directly affected by low
736 levels of the AID that in turn is reflected in lower SHM rate. The second reported a skewed λ
737 chain usage in B-1 cells (40). Based on these reports we propose a mechanistic model according
738 to which administration of TNF α antagonist blocks the TNF α on one hand and induces a vaccine-
739 like response on the other. Due to the TNF α blockade, immune response of B cells occurs extra
740 follicular where AID is downregulated, thus the encoded ADA exhibit lower SHM rates.
741 Moreover, the data suggests that the immune response following mAb administration may be a T
742 cell independent (TI) response which is governed by the B1 cell lineage with the characteristics
743 mentioned of an increased usage of λ light chains and little to non-evidence for SHM (40, 43).

744 Another possible mechanism that should be further explored is the strong TI immune response in
745 the marginal zone that is also induced by a drug/ADA immune-complex (IC). It was previously
746 suggested that many of the immune-mediated adverse effects attributed to ADA require the
747 formation of an IC intermediate that can have a variety of downstream effects (6, 44). In the
748 context of the system we investigated, administration of a TNF α antagonist will divert the
749 immune response extra follicular either by TNF α blockade or by the formation of an IC carrying
750 multiple mAbs that can induce the cross-linking of cognate BCR. The BCR of ADA-encoding B
751 cells will undergo co-clustering leading to their activation in the TI pathway.

752 In our study we examined molecular aspects related to the formation of ADA. To the best of our
753 knowledge, this is the first report describing ADA repertoire that resulted in insights about a
754 possible mechanism of ADA formation. Further work will be needed to elucidate additional
755 phenotypic markers of the B cells induced by mAb administration and the role of IC in the
756 activation of the B cell. Moreover, the mechanism described here covers the response to a TNF α -
757 antagonist, and by using the same omics approaches it will be highly informative to study the B
758 cell response following treatment with other mAbs.

759

760

761

762 **Acknowledgments**

763 **General:** We are grateful to George Georgiou for assisting with the LC-MS/MS measurements at UT Austin, for
764 Ulrich von Pawel-Rammingen from the Department of Molecular Biology, Umea University who kindly donated the
765 plasmid with the gene encoding the IdeS.

766 **Funding:** The work was partially supported by BSF grant 2017359 (Y.W.)

767 **Author contributions:** A.V.M, S.B.H, I.B. and Y.W. conceived the research. A.V.M. S.R. and Y.W. designed the
768 experiments, A.V.M., S.R., M.Y., E.F. and Y.D. performed experiments, A.V.M., S.R., S.B.H, M.Y., E.F., B.U. and
769 U.K. collected and processed clinical samples, A.V.M, A.K. and Y.W. carried out data analysis, A.V.M. and Y.W.
770 wrote the manuscript.

771 **Competing interests:** The authors declare no competing financial interests.

772 **This manuscript has been released as a Pre-Print at BioRxiv. DOI:**

773

References

References

1. Grilo AL, Mantalaris A. The Increasingly Human and Profitable Monoclonal Antibody Market. *Trends in biotechnology* (2019) 37(1):9-16. doi: 10.1016/j.tibtech.2018.05.014.
2. van Schouwenburg PA, Rispens T, Wolbink GJ. Immunogenicity of anti-TNF biologic therapies for rheumatoid arthritis. *Nat Rev Rheumatol* (2013) 9(3):164-72. doi: 10.1038/nrrheum.2013.4.
3. De Groot AS, Scott DW. Immunogenicity of protein therapeutics. *Trends in immunology* (2007) 28(11):482-90. doi: 10.1016/j.it.2007.07.011.
4. Hansel TT, Kropshofer H, Singer T, Mitchell JA, George AJ. The safety and side effects of monoclonal antibodies. *Nat Rev Drug Discov* (2010) 9(4):325-38. doi: 10.1038/nrd3003.
5. Bloem K, Hernandez-Breijo B, Martinez-Feito A, Rispens T. Immunogenicity of Therapeutic Antibodies: Monitoring Antidrug Antibodies in a Clinical Context. *Ther Drug Monit* (2017) 39(4):327-32. doi: 10.1097/FTD.0000000000000404.
6. Krishna M, Nadler SG. Immunogenicity to Biotherapeutics - The Role of Anti-drug Immune Complexes. *Frontiers in Immunology* (2016) 7. doi: 10.3389/fimmu.2016.00021.
7. Nelson AL, Dhimolea E, Reichert JM. Development trends for human monoclonal antibody therapeutics. *Nat Rev Drug Discov* (2010) 9(10):767-74. doi: 10.1038/nrd3229.
8. Ben-Horin S, Heap GA, Ahmad T, Kim H, Kwon T, Chowers Y. The immunogenicity of biosimilar infliximab: can we extrapolate the data across indications? *Expert Rev Gastroenterol Hepatol* (2015) 9 Suppl 1:27-34. doi: 10.1586/17474124.2015.1091307.
9. Bendtzen K. Immunogenicity of Anti-TNF- α Biotherapies: II. Clinical Relevance of Methods Used for Anti-Drug Antibody Detection. *Frontiers in Immunology* (2015) 6:109. doi: 10.3389/fimmu.2015.00109.
10. Putnam WS, Prabhu S, Zheng Y, Subramanyam M, Wang Y-MC. Pharmacokinetic, pharmacodynamic and immunogenicity comparability assessment strategies for monoclonal antibodies. *Trends in biotechnology* (2010) 28(10):509-16. doi: 10.1016/j.tibtech.2010.07.001.
11. Sands BE, Anderson FH, Bernstein CN, Chey WY, Feagan BG, Fedorak RN, et al. Infliximab maintenance therapy for fistulizing Crohn's disease. *New England Journal of Medicine* (2004) 350(9):876-85. doi: 10.1056/NEJMoa030815.
12. Mitoma H, Horiuchi T, Hatta N, Tsukamoto H, Harashima S, Kikuchi Y, et al. Infliximab induces potent anti-inflammatory responses by outside-to-inside signals through transmembrane TNF-alpha. *Gastroenterology* (2005) 128(2):376-92.
13. Ben-Horin S, Vande Casteele N, Schreiber S, Lakatos PL. Biosimilars in Inflammatory Bowel Disease: Facts and Fears of Extrapolation. *Clin Gastroenterol Hepatol* (2016) 14(12):1685-96. doi: 10.1016/j.cgh.2016.05.023.
14. Baker MP, Reynolds HM, Lumicisi B, Bryson CJ. Immunogenicity of protein therapeutics: The key causes, consequences and challenges. *Self Nonself* (2010) 1(4):314-22. doi: 10.4161/self.1.4.13904.
15. Ungar B, Engel T, Yablecovitch D, Lahat A, Lang A, Avidan B, et al. Prospective Observational Evaluation of Time-Dependency of Adalimumab Immunogenicity and Drug Concentrations: The Poetic Study. *The American journal of gastroenterology* (2018) 113(6):890-8. doi: 10.1038/s41395-018-0073-0.
16. Ungar B, Chowers Y, Yavzori M, Picard O, Fudim E, Har-Noy O, et al. The temporal evolution of antidrug antibodies in patients with inflammatory bowel disease treated with infliximab. *Gut* (2014) 63(8):1258-64. doi: 10.1136/gutjnl-2013-305259.

- 323 17. Vincent FB, Morand EF, Murphy K, Mackay F, Mariette X, Marcelli C. Antidrug
324 antibodies (ADAb) to tumour necrosis factor (TNF)-specific neutralising agents in chronic
325 inflammatory diseases: a real issue, a clinical perspective. *Ann Rheum Dis* (2013) 72(2):165-78.
326 doi: 10.1136/annrheumdis-2012-202545.
- 327 18. Tatarewicz S, Miller JM, Swanson SJ, Moxness MS. Rheumatoid factor interference in
328 immunogenicity assays for human monoclonal antibody therapeutics. *J Immunol Methods* (2010)
329 357(1-2):10-6. doi: 10.1016/j.jim.2010.03.012.
- 330 19. Bloem K, van Leeuwen A, Verbeek G, Nurmohamed MT, Wolbink GJ, van der Kleij D, et
331 al. Systematic comparison of drug-tolerant assays for anti-drug antibodies in a cohort of
332 adalimumab-treated rheumatoid arthritis patients. *J Immunol Methods* (2015) 418:29-38. doi:
333 10.1016/j.jim.2015.01.007.
- 334 20. Ben-Horin S, Chowers Y. Tailoring anti-TNF therapy in IBD: drug levels and disease
335 activity. *Nature reviews Gastroenterology & hepatology* (2014) 11(4):243-55. doi:
336 10.1038/nrgastro.2013.253.
- 337 21. Ben-Horin S, Yavzori M, Katz L, Kopylov U, Picard O, Fudim E, et al. The immunogenic
338 part of infliximab is the F(ab')₂, but measuring antibodies to the intact infliximab molecule is
339 more clinically useful. *Gut* (2010) 60(1):gut.2009.201533-48. doi: 10.1136/gut.2009.201533.
- 340 22. von Pawel-Rammingen U, Johansson BP, Björck L, IdeS, a novel streptococcal cysteine
341 proteinase with unique specificity for immunoglobulin G. *The EMBO Journal* (2002) 21(7):1607-
342 15. doi: 10.1093/emboj/21.7.1607.
- 343 23. Kopylov U, Mazor Y, Yavzori M, Fudim E, Katz L, Coscas D, et al. Clinical utility of
344 antihuman lambda chain-based enzyme-linked immunosorbent assay (ELISA) versus double
345 antigen ELISA for the detection of anti-infliximab antibodies. *Inflammatory bowel diseases*
346 (2012) 18(9):1628-33. doi: 10.1002/ibd.21919.
- 347 24. Lee J, Boutz DR, Chromikova V, Joyce MG, Vollmers C, Leung K, et al. Molecular-level
348 analysis of the serum antibody repertoire in young adults before and after seasonal influenza
349 vaccination. *Nature Medicine* (2016) 22(12):1456-+. doi: 10.1038/nm.4224.
- 350 25. Lavinder JJ, Wine Y, Giesecke C, Ippolito GC, Horton AP, Lungu OI, et al. Identification
351 and characterization of the constituent human serum antibodies elicited by vaccination.
352 *Proceedings of the National Academy of Sciences of the United States of America* (2014)
353 111(6):2259-64. doi: 10.1073/pnas.1317793111.
- 354 26. Haney DJ, Lock MD, Gurwith M, Simon JK, Ishioka G, Cohen MB, et al.
355 Lipopolysaccharide-specific memory B cell responses to an attenuated live cholera vaccine are
356 associated with protection against *Vibrio cholerae* infection. *Vaccine* (2018) 36(20):2768-73.
- 357 27. Davydov AN, Obratsova AS, Lebedin MY, Turchaninova MA, Staroverov DB, Merzlyak
358 EM, et al. Comparative Analysis of B-Cell Receptor Repertoires Induced by Live Yellow Fever
359 Vaccine in Young and Middle-Age Donors. *Front Immunol* (2018) 9:2309. doi:
360 10.3389/fimmu.2018.02309.
- 361 28. Blanchard-Rohner G, Pulickal AS, der Zijde CMJ-v, Snape MD, Pollard AJ. Appearance
362 of peripheral blood plasma cells and memory B cells in a primary and secondary immune
363 response in humans. *Blood* (2009) 114(24):4998-5002. doi: 10.1182/blood-2009-03-211052.
- 364 29. Avram O, Vaisman-Mentesh A, Yehezkel D, Ashkenazy H, Pupko T, Wine Y. ASAP, A
365 Webserver for Immunoglobulin-Sequencing Analysis Pipeline. *Frontiers in Immunology* (2018)
366 9. doi: 10.3389/fimmu.2018.01686.
- 367 30. Greiff V, Menzel U, Haessler U, Cook SC, Friedensohn S, Khan TA, et al. Quantitative
368 assessment of the robustness of next-generation sequencing of antibody variable gene repertoires
369 from immunized mice. *BMC immunology* (2014) 15(1):40. doi: 10.1186/s12865-014-0040-5.
- 370 31. Menzel U, Greiff V, Khan TA, Haessler U, Hellmann I, Friedensohn S, et al.
371 Comprehensive Evaluation and Optimization of Amplicon Library Preparation Methods for High-
372 Throughput Antibody Sequencing. *PLOS ONE* (2014) 9(5). doi: 10.1371/journal.pone.0096727.

- 373 32. Mroczek ES, Ippolito GC, Rogosch T, Hoi KH, Hwangpo TA, Brand MG, et al.
374 Differences in the composition of the human antibody repertoire by B cell subsets in the blood.
375 *Frontiers in immunology* (2014) 5:96-. doi: 10.3389/fimmu.2014.00096.
- 376 33. Volpe JM, Kepler TB. Large-scale analysis of human heavy chain V(D)J recombination
377 patterns. *Immunome research* (2008) 4:3-. doi: 10.1186/1745-7580-4-3.
- 378 34. Wine Y, Boutz DR, Lavinder JJ, Miklos AE, Hughes RA, Hoi KH, et al. Molecular
379 deconvolution of the monoclonal antibodies that comprise the polyclonal serum response. *Proc*
380 *Natl Acad Sci USA* (2013) 110(8):2993-8. doi: 10.1073/pnas.1213737110.
- 381 35. Ademokun A, Wu YC, Martin V, Mitra R, Sack U, Baxendale H, et al. Vaccination-
382 induced changes in human B-cell repertoire and pneumococcal IgM and IgA antibody at different
383 ages. *Aging cell* (2011) 10(6):922-30. doi: 10.1111/j.1474-9726.2011.00732.x.
- 384 36. Galson JD, Trück J, Fowler A, Clutterbuck EA, Münz M, Cerundolo V, et al. Analysis of
385 B Cell Repertoire Dynamics Following Hepatitis B Vaccination in Humans, and Enrichment of
386 Vaccine-specific Antibody Sequences. *EBioMedicine* (2015) 2(12):2070-9. doi:
387 <https://doi.org/10.1016/j.ebiom.2015.11.034>.
- 388 37. DeKosky BJ, Lungu OI, Park D, Johnson EL, Charab W, Chrysostomou C, et al. Large-
389 scale sequence and structural comparisons of human naive and antigen-experienced antibody
390 repertoires. *Proc Natl Acad Sci U S A* (2016) 113(19):E2636-45. doi: 10.1073/pnas.1525510113.
- 391 38. Boutz DR, Horton AP, Wine Y, Lavinder JJ, Georgiou G, Marcotte EM. Proteomic
392 Identification of Monoclonal Antibodies from Serum. *Analytical Chemistry* (2014) 86(10):4758-
393 66. doi: 10.1021/ac4037679.
- 394 39. Robinson JE, Hastie KM, Cross RW, Yenni RE, Elliott DH, Rouelle JA, et al. Most
395 neutralizing human monoclonal antibodies target novel epitopes requiring both Lassa virus
396 glycoprotein subunits. *Nature communications* (2016) 7:11544-. doi: 10.1038/ncomms11544.
- 397 40. Hayakawa K, Hardy RR, Herzenberg LA. Peritoneal Ly-1 B cells: genetic control,
398 autoantibody production, increased lambda light chain expression. *Eur J Immunol* (1986)
399 16(4):450-6. doi: 10.1002/eji.1830160423.
- 400 41. Rowley B, Tang L, Shinton S, Hayakawa K, Hardy RR. Autoreactive B-1 B cells:
401 constraints on natural autoantibody B cell antigen receptors. *J Autoimmun* (2007) 29(4):236-45.
- 402 42. Pasparakis M, Alexopoulou L, Episkopou V, Kollias G. Immune and inflammatory
403 responses in TNF alpha-deficient mice: a critical requirement for TNF alpha in the formation of
404 primary B cell follicles, follicular dendritic cell networks and germinal centers, and in the
405 maturation of the humoral immune response. *Journal of Experimental Medicine* (1996)
406 184(4):1397-411. doi: 10.1084/jem.184.4.1397.
- 407 43. Kantor AB, Herzenberg LA. Origin of murine B cell lineages. *Annu Rev Immunol* (1993)
408 11:501-38. doi: 10.1146/annurev.iy.11.040193.002441.
- 409 44. Bar-Yoseph H, Pressman S, Blatt A, Vainberg SG, Maimon N, Starosvetsky E, et al.
410 Infliximab-Tumor Necrosis Factor Complexes Elicit Formation of Anti-drug Antibodies.
411 *Gastroenterology* (2019) In Press. doi: 10.1053/j.gastro.2019.08.009.
- 412 45. Wenig K, Chatwell L, von Pawel-Rammingen U, Björck L, Huber R, Sondermann P.
413 Structure of the streptococcal endopeptidase IdeS, a cysteine proteinase with strict specificity for
414 IgG. *Proceedings of the National Academy of Sciences of the United States of America* (2004)
415 101(50):17371-6. doi: 10.1073/pnas.0407965101.
- 416 46. Cox J, Mann M. MaxQuant enables high peptide identification rates, individualized p.p.b.-
417 range mass accuracies and proteome-wide protein quantification. *Nature biotechnology* (2008)
418 26(12):1367-72. doi: 10.1038/nbt.1511.
- 419 47. Cox J, Hein MY, Lubner CA, Paron I, Nagaraj N, Mann M. Accurate proteome-wide label-
420 free quantification by delayed normalization and maximal peptide ratio extraction, termed
421 MaxLFQ. *Molecular & cellular proteomics : MCP* (2014) 13(9):2513-26. doi:
422 10.1074/mcp.M113.031591.

48. Cox J, Neuhauser N, Michalski A, Scheltema RA, Olsen JV, Mann M. Andromeda: a peptide search engine integrated into the MaxQuant environment. *Journal of proteome research* (2011) 10(4):1794-805. doi: 10.1021/pr101065j.

Figure legends

Figure 1: IFX digestion and IFX-F(ab')₂ purification. (A) Schematic representation of IgG digestion with IdeS. IdeS is a highly specific immunoglobulin-degrading enzyme that cleaves below the disulfide bonds in the IgG hinge region. The cleavage results in the production of IFX-F(ab')₂ fragment and two ½ Fc fragments. (B) SDS-PAGE analysis of intact IgG (lane 2), following IdeS digestion (lane 3) and purified IFX-F(ab')₂ following a 2-step affinity chromatography purification including protein A and kappa-select columns (lane 4). (C) Presence of Fc and intact IgG traces was measured by direct ELISA where intact IFX and purified IFX-F(ab')₂ were compared to a control antigen (streptavidin) as coating agents followed by direct incubation with an anti-Fc HRP conjugate at the detection phase. (D) The functionality of the recovered IFX-F(ab')₂ was confirmed by testing it for TNFα binding by ELISA in comparison to intact IFX. The ELISA setup included TNFα as the coating agent and anti- λ HRP conjugate at the detection phase. For panel C–D, triplicate averages were calculated as mean, with error bars indicating s.d.

Figure 2: Standard curve for ADA quantification in patients treated with IFX. ADA were purified from sera of 17 patients treated with IFX, utilizing consecutive affinity chromatography steps including protein G and custom made IFX-F(ab')₂ columns. (A) Purified ADA were tested in ELISA for functionality. TNFα was used as the coating agent followed by incubation with purified ADA and anti-Fc HRP conjugate at the detection phase. Control included serum obtained from a healthy donor. (B) SDS-PAGE analysis of intact IFX (lane 2) and purified ADA (lane 3). (C) The effect of serum on ADA standard was tested in ELISA by spiking-in differential concentrations of ADA into ADA negative serum.

Figure 3: AHLC and the newly developed mAb-F(ab')₂ based bio-immunoassay configuration and their application on serum samples from patients treated with IFX. (A) AHLC assay is based on an ELISA where TNFα is used as the coating agent, following the incubation with the mAb drug followed by serial dilutions of the tested sera. anti- λ HRP conjugate is used at the detection phase. (B) The newly developed mAb-F(ab')₂ based bio-immunoassay configuration. The assay is based on an ELISA where mAb-F(ab')₂ is used as the coating agent followed by serial dilutions of the tested sera. Anti-Fc HRP conjugate is used at the detection phase. (C) ELISA obtained by utilizing the AHLC assay on two serum samples. Using this assay, one of the tested sera showed detectable levels of ADA (AHLC⁽⁺⁾) and one had no detectable levels of ADA (AHLC⁽⁻⁾). (D) Both serum samples were tested by the newly developed mAb-F(ab')₂ based bio-immunoassay. This assay was able to detect ADA in both sera. For C–D, averages were calculated as mean from triplicates, with error bars indicating s.d.

Figure 4: Configuration of the assay for determining the neutralization index of ADA in patient sera and competitive ELISA between ADA and rhTNFα. (A) The newly developed mAb-F(ab')₂ based bio-immunoassay configuration (left) and the modified configuration where mAb-F(ab')₂ binding site is blocked by saturating the assay with rhTNFα (right). (B) Competitive effect of rhTNFα on ADA binding to IFX-F(ab')₂. ELISA plate was coated with 5μg/ml of IFX-F(ab')₂. ADA standard was diluted 3-fold in blocking solution supplemented with 5nM rhTNFα. ADA diluted 3-fold in blocking solution without the presence of rhTNFα served as a control.

Figure 5: Neutralization index ELISA. (A) Graph representing the ELISA results obtained utilizing the neutralization assay on serum sample that show detectable levels of ADA (AHLC⁽⁺⁾) and (B) serum sample with no detectable levels of ADA (AHLC⁽⁻⁾). (C) Scatter plot consolidating the neutralization index obtained by applying the immunoassay on sera from 55 patients treated with IFX (****P* = 0.0003, Mann-Whitney *U* test). For B–C, averages were calculated as mean, with error bars indicating s.d.

Figure 6: V, D and J family usage in B cell following IFX infusion. mBC and PB from a patient treated with IFX were collected at two time points (D0, D10) and processed for NGS analysis. The V family usage showed no difference between D0 and D10, different B cell subsets and isotypes. The D and J family usage showed no difference between time points.

Figure 7: CDRH3 length at two time point and across isotypes. PB from a patient treated with IFX were collected at two time points (D0, D10) and processed for NGS analysis. An increase in antibody CDRH3 length was observed. (****P* < 0.001, Mann-Whitney *U* test).

980 **Figure 8: Somatic hyper mutations.** PB from a patient treated with IFX were collected at two time points (D0, D10)
 981 and processed for NGS analysis. A decrease in the number of Ka mutations (number of non-synonymous mutation
 982 per codon) and Ks mutations (number of synonymous mutations per codon) was observed at D10. (**** $P < 0.0001$,
 983 Mann-Whitney U test).
 984

985 **Figure 9: V-gene and circulating antibody repertoire characteristics.** (A) The V(D)J family usage of V-gene
 986 sequences that were identified by LC-MS/MS. (B) Mapping of V-gene sequences to B cell subsets and (C) isotypes,
 987 based on NGS data.
 988

989 **Table 1: ADA concentrations in 55 serum samples from patients treated with IFX.** Serum samples were initially
 990 stratified into AHLC (+) and AHLC (-) based on the AHLC assay used in the clinic. The newly developed bio-
 991 immunoassay for the quantification of total ADA was applied on all serum samples and concentration are listed. All
 992 ADA concentrations are in $\mu\text{g/ml}$.
 993

AHLC ⁽⁻⁾ patients			AHLC ⁽⁺⁾ patients		
Patient #	AHLC	New bio-immunoassay $\mu\text{g/ml}$	Patient #	AHLC	New bio-immunoassay $\mu\text{g/ml}$
5645	0	867.33	14655	7.9	121.95
5557	0.9	0	15046	16.6	85.24
5381	1.9	0	15460	21.1	147.89
6497	1.6	26.26	15809	22.8	996.84
6386	1.7	0	15107	6.3	126.5
6259	0.8	41.39	14408	4.8	90.54
6098	1.3	0	4297	8.9	274.6
5993	1.3	0	5048	5.6	49.28
5912	1.8	0	5735	6.9	99.67
5882	1.7	152.72	6393	3.4	289.31
5822	1.3	0	6324	6.7	91.14
6291	0.7	19.43	6275	31.8	242.03
6616	0.3	84.05	6261	27.2	245.52
7083	1	97.29	6208	5.8	65.35
7041	1	0	6165	3	2.7
7004	0.7	4.28	6148	7.2	148.88
6866	1.3	80.05	9348	42.2	285.05
6788	1.8	46.83	8970	59.3	1268.5
6740	1.5	0	8816	27.2	396.2
14735	0.4	0	7553	46.7	178.83
14752	1.2	43.87	12113	20.9	772.83
14879	1.7	0	12104	20.9	441.09
14834	0.57	0	6329	11	87.31
13741	1.3	18	8178	7.9	55.11
13711	0.3	0	7653	16.1	53.52
14278	1.72	0	8856	42.4	87.97
			9454	7.8	265.35
			12343	16.5	358.54
			12345	37	329.49

994 **Table 2: B cell frequency of a patient treated with IFX.**

Time point	B cell subset	% Frequency of sorted cells (out of CD19+ cells)	No. of raw paired-end sequencing reads		No. of filtered paired-end sequencing reads			No. of unique IGH clonotypes extracted (Unique CDRH3)
			Replicate A	Replicate B	Replicate A	Replicate B	Joint	
D0	PB	0.9%	39,129	63,168	12,863	19,082	2041	1294
	mBC	10%	714,722	639,984	121,998	111,373	30,725	9146
D10	PB	11.5%	167,859	151,849	49,762	46,192	10,341	5590
	mBC	9.7%	528,765	488,619	143,864	133,879	40,899	19,521

995
996
997
998

Table 3: Summary of identified peptides and the corresponding clonotype and antibody somatic variances in the LC-MS/MS spectra. E: elution, FT: flow-through.

	Day 0	Day 10
Total peptides	908	3177
Total antibody peptides	761	2805
Total CDRH3	42	224
Present in ≥ 2 technical replicates	30	166
Frequency ratio E/FT > 5	11	81
N ^o of clones	5	62
N ^o of somatic variances	35	205

999
1000
1001
1002
1003
1004
1005
1006
1007
1008
1009
1010
1011
1012
1013
1014
1015

Figure 1

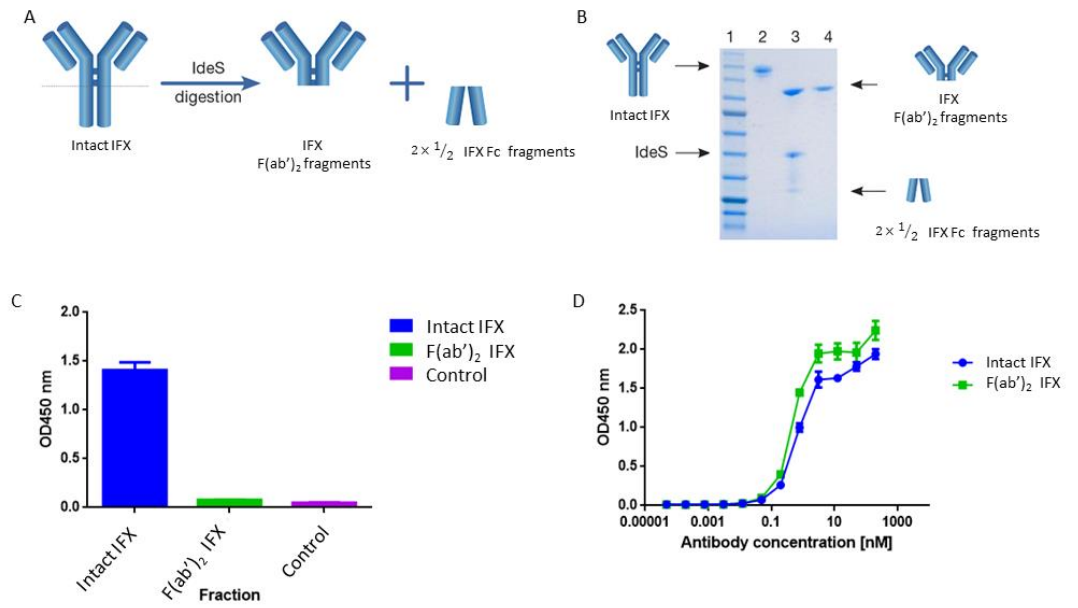


Figure 2

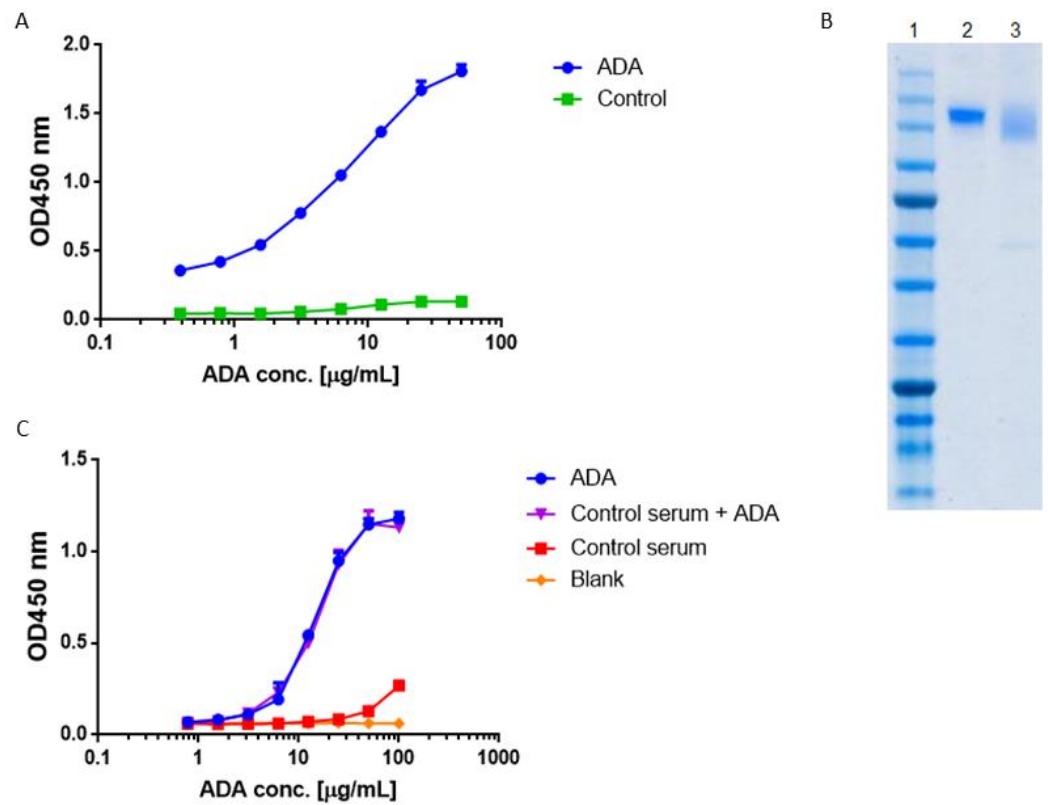


Figure 3

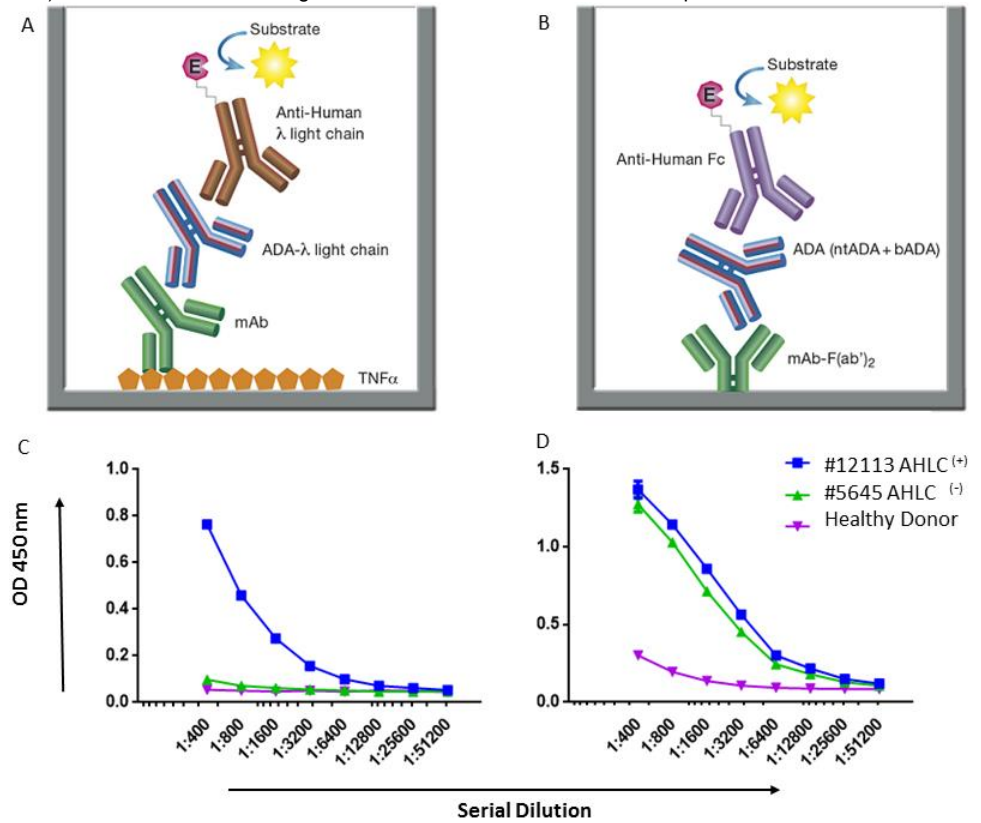


Figure 4

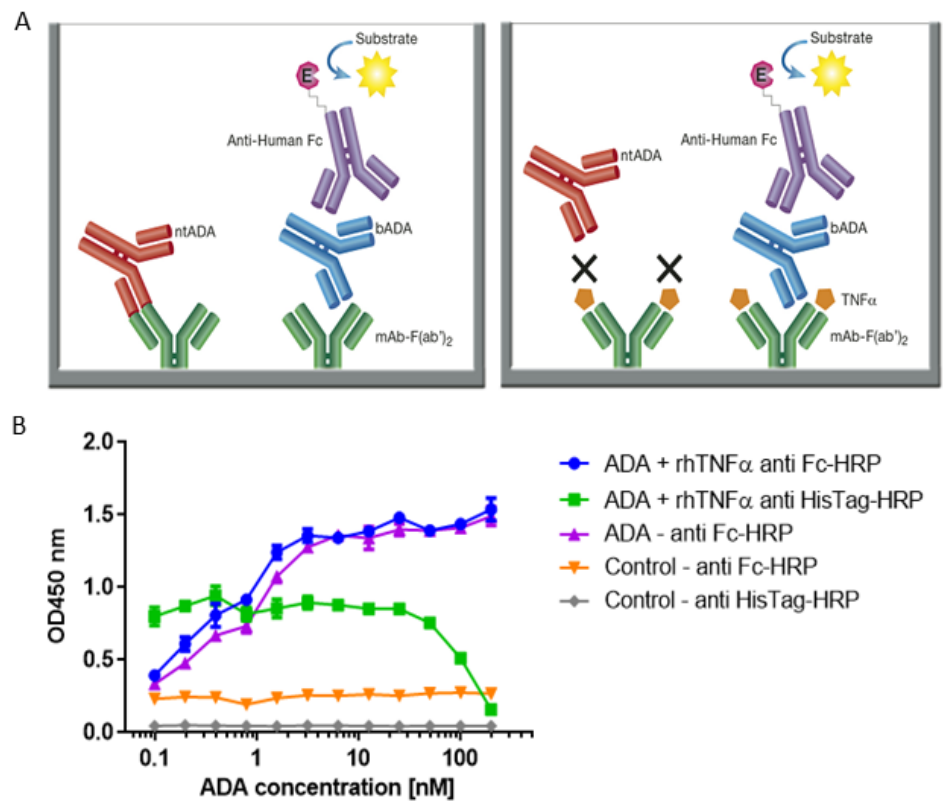


Figure 5

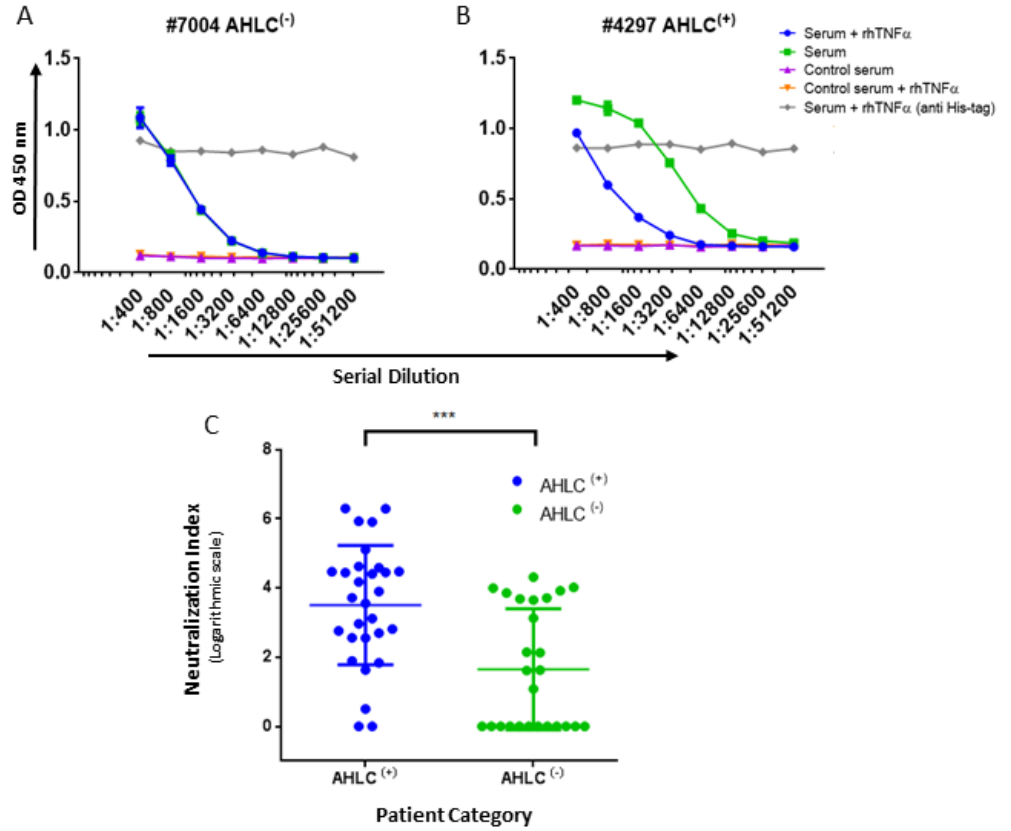


Figure 6

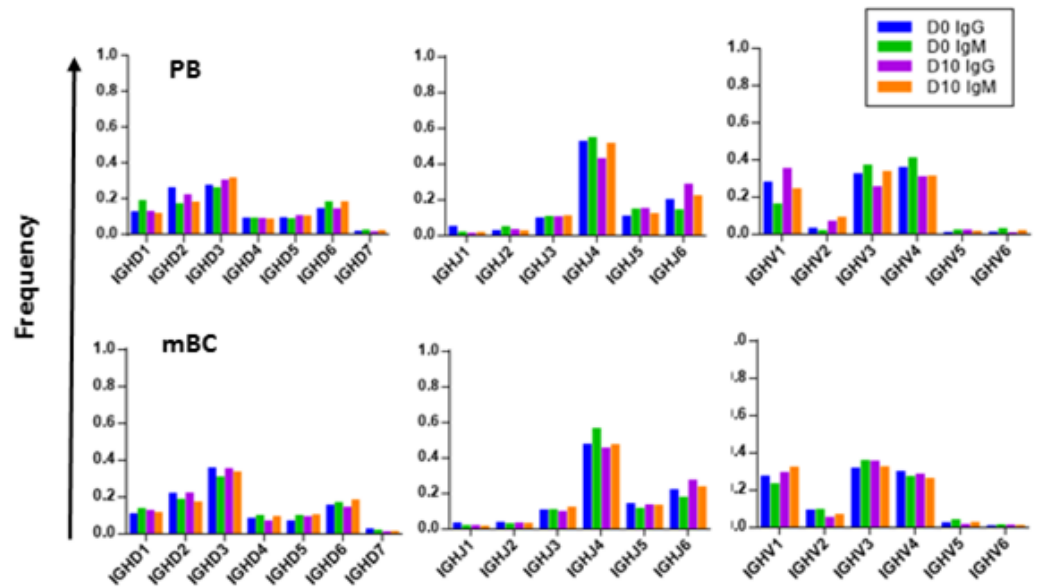


Figure 7

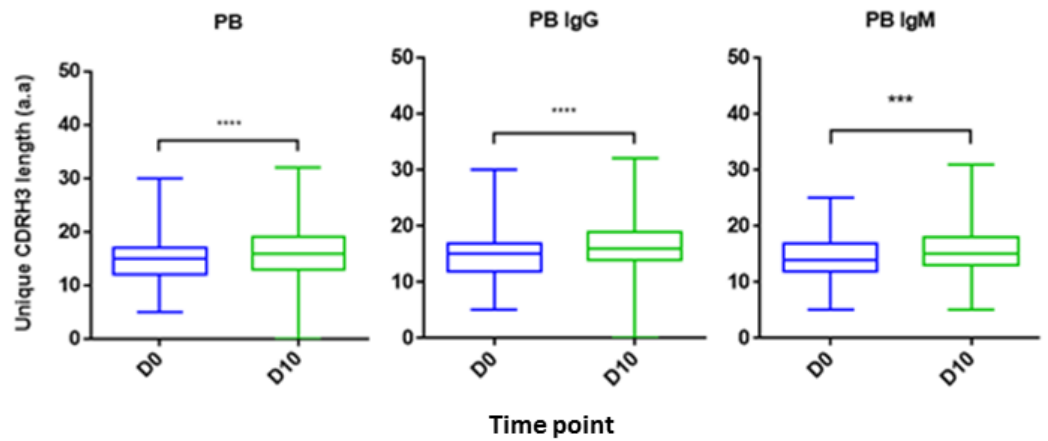


Figure 8

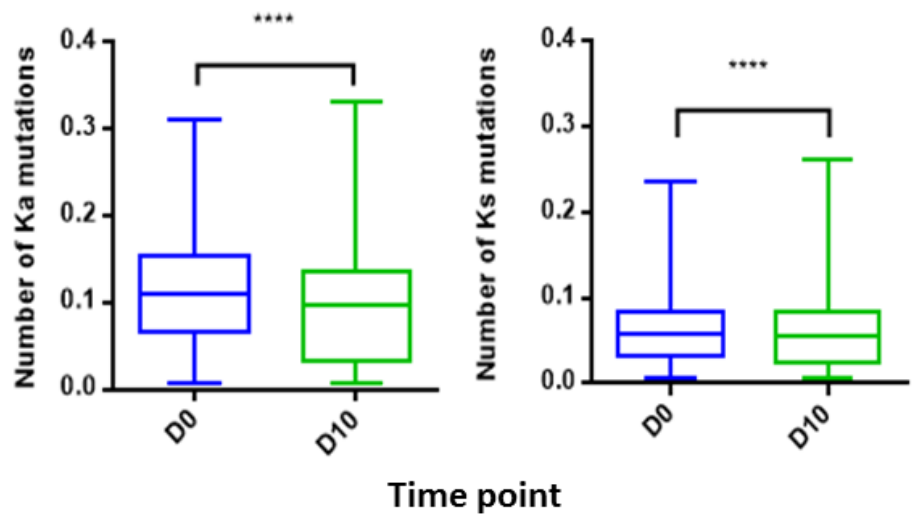


Figure 9

